

Fatigue Approach for WAPS

Auteur : Romar Borzacchiello, Guilherme

Promoteur(s) : 14956

Faculté : Faculté des Sciences appliquées

Diplôme : Master : ingénieur civil mécanicien, à finalité spécialisée en "Advanced Ship Design"

Année académique : 2020-2021

URI/URL : <http://hdl.handle.net/2268.2/13280>

Avertissement à l'attention des usagers :

Tous les documents placés en accès ouvert sur le site le site MatheO sont protégés par le droit d'auteur. Conformément aux principes énoncés par la "Budapest Open Access Initiative"(BOAI, 2002), l'utilisateur du site peut lire, télécharger, copier, transmettre, imprimer, chercher ou faire un lien vers le texte intégral de ces documents, les disséquer pour les indexer, s'en servir de données pour un logiciel, ou s'en servir à toute autre fin légale (ou prévue par la réglementation relative au droit d'auteur). Toute utilisation du document à des fins commerciales est strictement interdite.

Par ailleurs, l'utilisateur s'engage à respecter les droits moraux de l'auteur, principalement le droit à l'intégrité de l'oeuvre et le droit de paternité et ce dans toute utilisation que l'utilisateur entreprend. Ainsi, à titre d'exemple, lorsqu'il reproduira un document par extrait ou dans son intégralité, l'utilisateur citera de manière complète les sources telles que mentionnées ci-dessus. Toute utilisation non explicitement autorisée ci-avant (telle que par exemple, la modification du document ou son résumé) nécessite l'autorisation préalable et expresse des auteurs ou de leurs ayants droit.



With the support of the
Erasmus+ Programme
of the European Union



Fatigue Approach for WAPS

submitted on 02 August 2021

by

Romar Borzacchiello, Guilherme | Im Steinfeld 4 | 61440 Oberursel | guilhermeromar@gmail.com

Student ID No.: 220 202 361

Supervisor:

Dr.-Ing. Jörg Peschmann

DNV GL SE

Hamburg

Germany

Reviewer:

Dr. Maciej Taczala

West Pomeranian University of Technology

Szczecin

Poland

This page is intentionally left blank

DECLARATION OF AUTORSHIP

I, Guilherme Romar Borzacchiello, declare that this thesis and the work presented in it are my own and have been generated by me as the result of my own original research.

“Fatigue Approach for WAPS”

Where I have consulted the published work of others, this is always clearly attributed.

Where I have quoted from the work of others, the source is always given. With the exception of such quotations, this thesis is entirely my own work.

I have acknowledged all main sources of help.

Where the thesis is based on work done by myself jointly with others, I have made clear exactly what was done by others and what I have contributed myself.

This thesis contains no material that has been submitted previously, in whole or in part, for the award of any other academic degree or diploma.

I cede copyright of the thesis in favour of the University of Rostock

Date:

Signature:

This page is intentionally left blank

ABSTRACT

In the context of climate change and limiting the global temperature rise, wind assisted propulsion systems (WAPS) appear as innovative emission reduction mechanisms, utilizing the thrust force generated by the wind to reduce fuel consumption. So, to assure the safety for the vessel and the equipment, these must follow a series of standards and guidelines, defined by classification societies not only to guide and ease their work, but also to assist the designer in evaluating the equipment's robustness. The implementation of such equipment, however, require new standards, because, although previous knowledge with structures mounted on ships may be useful, WAPS differ from many of them regarding the fact that they are in operation while the ship is navigating. Moreover, since WAPS rely on wind to operate, wind loads should also be considered carefully.

This complex problem can be extended for the whole WAPS, but, since such systems vary considerably, this would require an individual analysis. However, the connection between system and ship can be regarded as similar for most cases and, for this reason, a standard approach could be developed. Therefore, the present work, then, aimed to identify the relevant loads for fatigue in WAPS and to develop a standard approach for estimating fatigue damage for these systems in a rule context, focusing on the attachment of the WAPS to the hull.

A review on WAPS and on their present rules was carried to understand how such systems work and how the problem should be approached. Moreover, similarities to offshore wind turbines were drawn to better explore the problem, also considering further aspects relevant for a moving ship. The basis for the work was completed with an overview of the general fatigue assessment procedure.

Then, the loads and stresses acting on WAPS, resulting from winds and waves, as well as their combination, were approached at different levels of complexity. This required a series of assumptions to be made and proved for calculating the loads their combinations for the different procedures and levels of detail. In the end, the whole knowledge was gathered and summarized to present a fatigue approach for WAPS.

Keywords: Fatigue, Wind Assisted Propulsion Systems.

This page is intentionally left blank

CONTENTS

ABSTRACT	v
1. INTRODUCTION	1
1.1. Background.....	1
1.2. Mission	2
1.3. Goals.....	4
1.4. Organization	4
2. REVIEW AND BACKGROUND ON WAPS	5
2.1. Physics of Sailing	6
2.1.1. Wind Velocity Triangle.....	6
2.1.2. Equilibrium Conditions	8
2.2. WAPS Overview	11
2.2.1. Rotor Sails	11
2.2.2. Rigid Wing Sails	12
2.2.3. Soft Wing Sails.....	13
2.2.4. Soft Sail Systems - DynaRig.....	14
2.2.5. Ventilated Foil Systems	15
2.3. Fatigue for WAPS	16
2.3.1. Rules and Limitations.....	17
2.3.2. Offshore Wind Turbines Experience.....	19
2.3.3. Other Factors	21
3. FATIGUE	26
3.1. Fatigue Approaches and Stress Assessment.....	27
3.2. Fatigue Stress Range	28
3.2.1. Scantling Approach Factor, f_c	30
3.2.2. Environmental Factor, f_e	30
3.2.3. Mean Stress Factor, f_{mean}	30

3.2.4.	Thickness Effect, f_{thick}	30
3.2.5.	Material Factor, f_{material}	31
3.2.6.	Post Weld Treatment Factor, f_w	31
3.2.7.	Misalignment Factor, K_m	31
3.2.8.	Stress Range Spectrum	32
3.3.	Fatigue Strength Assessment	34
3.3.1.	S-N Curves	34
3.3.2.	Fatigue Damage	37
4.	FATIGUE LOADS AND STRESS RANGES	39
4.1.	Inertial Loads	40
4.1.1.	Envelope Accelerations	40
4.1.2.	Equivalent Design Approach	42
4.1.3.	Direct Hydrodynamics Calculation	44
4.2.	Wind loads	44
4.2.1.	Global Wind Matrix	44
4.2.2.	Wind Profile	45
4.2.3.	Gust Factor	47
4.2.4.	Vessel Speed	54
4.2.5.	Apparent Wind Heading and Speed	54
4.2.6.	Wind Load Application	55
4.2.7.	Wind Correction due to Obstructions	57
4.2.8.	Induced Wind by Ship Motions	58
4.2.9.	Shielding and Amplification Effects	58
4.2.10.	WAPS in Operational and Non-operation Modes	58
5.	LOAD COMBINATION	60
5.1.	Load Combination Methods	63
5.1.1.	Simple Superposition	63

5.1.2.	Simplified Correlation.....	63
5.1.3.	Direct Analysis.....	65
5.2.	Stress Combination.....	67
6.	FATIGUE ASSESSMENT FOR WAPS	69
7.	CONCLUSION.....	72
8.	ACKNOWLEDGEMENTS.....	74
9.	REFERENCES	75
	ANNEX.....	78

LIST OF FIGURES

Figure 1 – Wind velocity triangle downwind (NauticEd, 2013).....	7
Figure 2 – Wind velocity triangle upwind (NauticEd, 2013).....	7
Figure 3 – Sailing forces equilibrium, adapted from (Marchaj, 1982)	8
Figure 4 – Resultant aerodynamic forces (Fakiolas, 2020).....	8
Figure 5 – Boat sailing steadily on the wind (Püschl, 2018).....	9
Figure 6 – Different sails and their lift coefficients (Mathis Ruhl Architecture Navale)	10
Figure 7 – Rotor sail thrust generation (Fakiolas, 2020).....	11
Figure 8 – M/V Copenhagen (Noresepower, 2020).....	12
Figure 9 – Windship Technology rigid wing sails (Ovcina, 2021).....	13
Figure 10 – Oceanwings (Ayro, 2021).....	13
Figure 11 – Oceanwings installed in prototype (Ayro, 2021).....	14
Figure 12 – WISAMO inflatable sails (Michelin, 2021)	14
Figure 13 – Maltese Falcon (Maltese Falcon, 2020).....	15
Figure 14 – WASP Ecoliner (Dykstra, n.d.)	15
Figure 15 – Retrofitted Ventifoils installed (eConowind)	16
Figure 16 – WAPS approached by DNVGL-ST-0511 (DNV-GL, 2020).....	17
Figure 17 – Fatigue stress spectra (DNVGL-ST-0377, 2018)	18
Figure 18 – Definition of ship motions (DNV-RU-SHIP Pt.3 Ch.4, 2021).....	22
Figure 19 – Stress history (schematic) (Fricke W., 2017).....	26
Figure 20 – Stress history from on-board measurement (Fricke W., 2017).....	26
Figure 21 – Standard stress range spectra (DNVGL-ST-0377, 2018) [4.6.5]	33
Figure 22 – FAT class S-N curves with FAT X number (DNVGL-CG-0129, 2019) Sec.2 [2.3]	35
Figure 23 – S-N curves in air (DNVGL-CG-0129, 2019) Sec.2 [2.3]	36
Figure 24 – Palmgren-Miner's rule for stress spectrum (Fricke, Petershagen, & Paetzold, 1997).....	37
Figure 25 – Load history and reversals	50
Figure 26 – Rainflow matrix histogram (cycle average x cycle range)	50
Figure 27 – Spectrum A for inertial loads, adapted from (DNVGL-ST-0377, 2018).....	60
Figure 28 – Relevant stress range spectra, adapted from (DNVGL-ST-0377, 2018).....	61
Figure 29 – Standard stress range spectra (DNVGL-ST-0377, 2018) [4.6.5]	61
Figure 30 – Wave headings, 45° resolution (8 headings)	64
Figure 31 – Wind headings, 5° resolution (36 headings).....	64
Figure 32 – Flow diagram for component stochastic fatigue calculations (DNVGL-CG-0129, 2019).....	66
Figure 33 – Flow diagram for full stochastic fatigue calculations (DNVGL-CG-0129, 2019)67	

LIST OF TABLES

Table 1 – S-N parameters for air (DNVGL-CG-0129, 2019) Sec.2 [2.3].....	36
Table 2 – Load combinations for envelope accelerations, from (DNV-RU-SHIP Pt.3 Ch.4, 2021) Section 3 [3.3.4]	40
Table 3 – Load combination factors for HSM, HSA and FSM load cases, (DNV-RU-SHIP Pt.3 Ch.4, 2021) Sec.2 [2.2.1]	43
Table 4 – Load combination factors for BSR and BSP load cases, (DNV-RU-SHIP Pt.3 Ch.4, 2021) Sec.2 [2.2.1]	43
Table 5 – Load combination factors for OST and OSA load cases, (DNV-RU-SHIP Pt.3 Ch.4, 2021) Sec.2 [2.2.1]	44
Table 6 – Fatigue Gust Factor calculated for 10s (100 repetitions)	52
Table 7 – Fatigue Gust Factor calculated for 10m height (100 repetitions), T4 stands for roll period.....	53
Table 8 – Fatigue Gust Factor obtained by formula, T4 stands for roll period.....	54
Table 9 – Moment comparison for rectangular sails.....	56
Table 10 – Moment comparison for triangular sails	56
Table 11 – Normalized global wind chart showing the probability of wind conditions relative to the ship's heading along the main global trading routes	78

1. INTRODUCTION

1.1. Background

Climate change is real, and its effects can already be noticed in the increased frequency and magnitude of extreme weather events. The concentration of greenhouse gases (GHG) in the earth's atmosphere has been rising steadily and mean global temperatures along with it. Such scenario is caused, principally, by human activities, which contribute to the increase of carbon dioxide's concentration by burning fossil fuels (United Nations, 2021).

To avoid even more dramatic consequences, the Paris Agreement on climate change was agreed in 2015 by Parties to the United Nations Framework Convention on Climate Change and entered into force in 2016. Its central aim is to strengthen the global response to the threat of climate change by limiting the global temperature rise to no more than 2°C above pre-industrial levels and to pursue efforts to limit the temperature increase even further to 1.5°C (IMO Environmental Committee, 2021) (United Nations, 2021). Such agreement does not include international shipping, even it represents a considerable share in greenhouse gases emissions.

However, maritime transport plays an important role in worldwide trades and economy, and International Maritime Organization (IMO), as the regulatory body for the industry, is committed to reducing greenhouse gas emissions from international shipping. According to a study conducted by IMO in 2020, total shipping emitted 1,056 million tonnes of CO₂ in 2018, representing about 2.89% of the total global anthropogenic CO₂ emissions for that year. To change this scenario, more recent strategies outlined by IMO aim to stimulate investment not only in the development of low-carbon and zero-carbon fuels, but also of innovative energy efficient technologies (IMO, 2021).

In its strategy, IMO commits to reduce GHG emissions from international shipping, phasing them out as soon as possible still in this century. For such, there are different levels of ambition to guide the actions and to achieve goals gradually, first trying to stop the increase in GHG emissions and, next, reducing them by at least 50% by 2050 compared to 2008. In this sense, the strengthening of the energy efficiency design requirements for each phase will be necessary for the decline of the carbon intensity of the ship (IMO Environmental Committee, 2021).

Following this idea, IMO has also adopted mandatory measures to control and reduce emissions of greenhouse gases from international shipping. Two of them stand out: the Energy Efficiency Design Index (EEDI) mandatory for new ships, and the Ship Energy Efficiency Management Plan (SEEMP). The first one requires new ships to comply with minimum mandatory energy efficiency performance levels, while the last establishes a mechanism to improve the energy efficiency of ships through operational measures (IMO, 2021).

However, it is important to notice that the targets agreed in the initial IMO GHG strategy will not be met using fossil fuels and that investments towards innovative sustainable technologies, as well as alternative fuels, will be necessary to achieve the overall ambition. Within short to mid-term measures, it is possible to identify the initiation and support of research and development activities addressing marine propulsion and new technologies to enhance even more the energy efficiency of ships (IMO Environmental Committee, 2021). In this context, wind assisted propulsion systems (WAPS) appear as innovative emission reduction mechanisms, utilizing the thrust force generated by the wind to reduce fuel consumption.

Although alternative fuels present themselves as a clean energy source, they still struggle in terms of availability and competitiveness. Moreover, the utilization of different fuels requires engine conversion and, sometimes, even the construction of a new supply infrastructure. WAPS, on the other hand, can be installed in a variety of existing vessels without changing the prime-mover configuration and they rely on an inexhaustible and “free” energy source, available from the environment: wind.

Even if not every sea route has the right wind conditions for such a solution, it makes ecological and economic sense to utilize those systems to reduce fuel consumption. In fact, the presence of a WAPS does not exclude any modification regarding alternative fuels and engines, working as a complementary tool to achieve higher efficiency. More than this, those systems can be combined to eco-friendly engines and other solutions to reach a GHG-neutral operation (DNV, 2020).

1.2. Mission

To assure the safety for the vessel and the equipment, these must follow a series of standards and guidelines. Such are defined by classification societies, even as rules, not only to guide

and ease their work, but also to assist the designer in evaluating the equipment's robustness. They comprehend ultimate and fatigue strength, maximum and regular loads, vibrations, and other possible problems faced by the vessel or the equipment regarding structural strength.

The implementation of such equipment, however, will require new standards, which are still under development. Although previous knowledge with structures mounted on ships may be useful, WAPS differ from many of them regarding the fact that they are in operation while the ship is navigating. Moreover, since WAPS rely on wind to operate, wind loads should also be considered carefully.

In this sense, if calculating the most extreme situations for those systems is not much different from other ships and offshore structures, the consideration of inertial loads combined with wind loads presents a new challenge for assessing the fatigue damage. There is no guarantee that these loads are in phase, present the same frequency of occurrence or act on the same direction. Hence, the combination of both loads can be tricky, with their simple superposition resulting in too conservative damage estimations, while analysing them individually underestimates the damage as fatigue presents an exponential relation to stress ranges.

Therefore, a standard procedure to estimate fatigue damage for such systems would be very helpful. And this should be supported by previous existing class rules and standards, adapted to fit this situation, easing its application and comprehension.

The present work, then, aims to identify the relevant loads for fatigue in WAPS and to develop a standard approach for estimating fatigue damage for these systems in a rule context. Such complex problem can be extended to the whole WAPS structure, but this would require a more detailed and individual analysis, which is not the aim of the present work. A more detailed analysis can be interesting for the designer, even working with the classification society for that, but the idea here is to work on a common approach for those different systems that behave on distinct ways when exposed to wind.

Therefore, the focus is on the attachment of the WAPS to the hull, generally a support or pedestal to sustain the sail. The connection between system and ship can be regarded as similar for most cases and, for this reason, a standard approach may be developed. For this, according to the level of design and detail, different analyses can be applied and later compared for estimated fatigue damage.

1.3. Goals

To achieve the proposed mission, a set of goals can be outlined:

- Understand how different Wind Assisted Propulsion Systems work
- Review fatigue assessment rules and procedures, also pointing the present limitations regarding WAPS
- Identify relevant loads for fatigue in such systems and understand how they should be estimated, stressing out what needs to be considered and/or neglected
- Understand how stress can be assessed for fatigue
- Establish a procedure for combining the stresses arising from distinct loads
- Propose a common approach for assessing fatigue for WAPS

1.4. Organization

The first part of the thesis (Chapter 2) aims to give an overview of the wind propulsion assisted systems and to present the main difficulties to calculate fatigue for such equipment. Some examples are shown and the present rules are also presented. Similarities to offshore wind turbines are drawn to better explore the problem and considerations regarding the WAPS are made.

In the sequence (Chapter 3), there is a general explanation of the fatigue assessment procedure. The aim is to demonstrate the general principles that guide fatigue analysis and understand how stresses are accounted in to estimate the fatigue life. Several factors affecting the stress range estimation are also explained.

The loads and stress assessments for WAPS are explained in the following (Chapters 4). Those are described for different levels of refinement, from simple analysis to more complex ones. For this, there are some assumptions to be made and to be proved, establishing a standard procedure to assess the referred loads.

Once the loads and stresses are clarified, their combination is approached (Chapter 5). Again, different methods are presented to work at different levels of detail. Considerations on how such work should be performed are also stated.

Finally, the whole procedure is summarized in order to give an overview and better understanding of the developed approaches (Chapter 6).

2. REVIEW AND BACKGROUND ON WAPS

Wind propulsion is, for sure, no novelty in the maritime world. Humans have been sailing since much before understanding the physics behind this activity and for thousands of years wind provided the main moving force for ships. This only changed during the 19th century with the development of steam ships and, later, of those powered by oil. They were faster and more reliable to meet the trade schedule, what made commercial ships to gradually abandon sails.

The low bunker prices relegated alternative propulsion systems to a marginal existence, but sails, even though, were not fully left aside and their technologies have been under constant development. Competitive situations in the racing circuits such as the America's Cup pushed the evolution of rigid wing sails, for example, while the needs generated for shorthanded automated sailing led to the emergence of the DynaRig. Besides, the merchant shipping industry has recently revisited some previous ideas, as Flettner rotors (rotating sail) (DNV-GL, 2020).

However, the adoption of alternative propulsion systems is not only an economical question anymore, but also an ecological one. Wind propulsion systems can act as a complement, assisting the main propulsion systems, thus reducing fossil fuel consumption and, by consequence, reducing carbon footprint. WAPS can be operated under favourable conditions, providing these gains, while the main engines would guarantee that the ship will meet the schedule.

In this sense, there are already some alternatives at use, while many new ideas are emerging. These systems can be very different one from another and the choice for a particular WAPS will depend on the ship, the route and the operation of the WAPS itself. Therefore, the present chapter aims to explain how WAPS works and to present an overview of the current design for these systems.

Moreover, the present approach for fatigue in WAPS will be showed to discuss its limitations. This will also be compared to fatigue analyses for offshore wind turbines, which are similarly exposed to wind and wave loads. By last, possible difficulties in the analysis will be discussed to narrow the scope and justify the future considerations for simplification of the problem.

2.1. Physics of Sailing

Even though vessels with WAPS behave differently from sailing vessels, knowing the physics behind sailing is fundamental to understand how wind propulsion systems work. Basically, sailing consists utilizing sails to generate a driving force from the wind to overcome the resistance to motion. As the vessel moves through the fluids, sails and hull develop drag and lift as they split wind and water into two flows that travel at different speeds, causing a pressure difference.

However, it is important to notice that both resistance and driving forces arise from two different flow fields: one in the water, another one in the air. And the equilibrium of forces should happen in both fields. Therefore, the resultant force comes from the interaction among hull and rig resistance, driving power of sails and stability (Reche, 2020).

2.1.1. Wind Velocity Triangle

The driving force, as said before, comes from the wind; more exactly, it arises from the force generated by the apparent wind on sails. The boat is moving along a sailing direction at a defined speed, with an angle in relation to true wind speed vector, from the environment. The combination of these two vectors results in the apparent wind speed, the one felt on-board.

It is easy to notice that, except when the vessel is not moving, true wind and apparent wind will present different magnitudes and directions in relation to the ship. While the first one can be regarded as constant, the second one is the vector sum of the true wind velocity minus the boat speed, depending, then, always on sailing direction and speed. This relation between true wind, ship sailing speed and apparent wind is better shown in the wind velocity triangle (Figure 1 and Figure 2).

Apparent wind speed (AWS) and angle (AWA) can be, therefore, written from trigonometrical relations. The speed is deducted from true wind speed (TWS), true wind angle (TWA) and vessel speed (V_s), utilizing the law of cosines, leading to equations 1 and 2:

$$AWS = \sqrt{V_s^2 + TWS^2 + 2 * V_s * TWS * \cos (TWA)} \quad (1)$$

$$AWA = \arccos \left(\frac{TWS * \cos(TWA) + V_s}{AWS} \right) \quad (2)$$

Ship's heading is fundamental for the shape of the wind velocity triangle as the angle between vessel and true wind affect directly the corresponding apparent wind speed. For example, when sailing pure downwind (TWA = 180°), boat and true wind speeds are summed up (Figure 1); while sailing pure upwind (TWA = 0°) means that the vessel's speed should be subtracted from the true wind one (Figure 2).

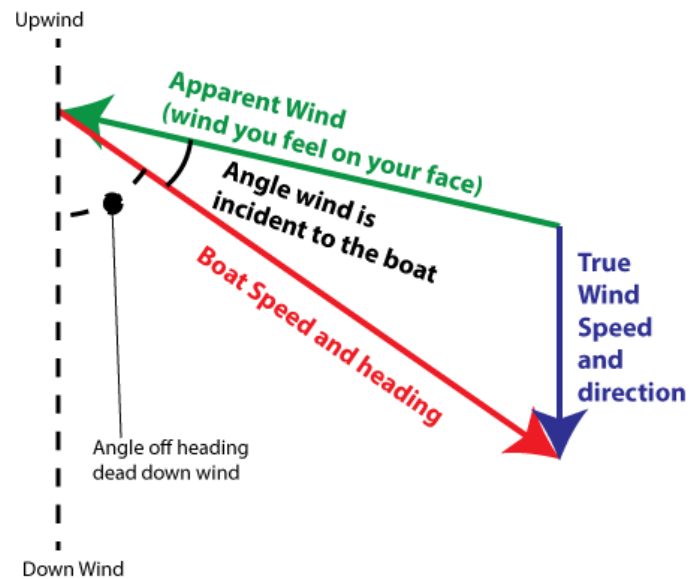


Figure 1 – Wind velocity triangle downwind (NauticEd, 2013)

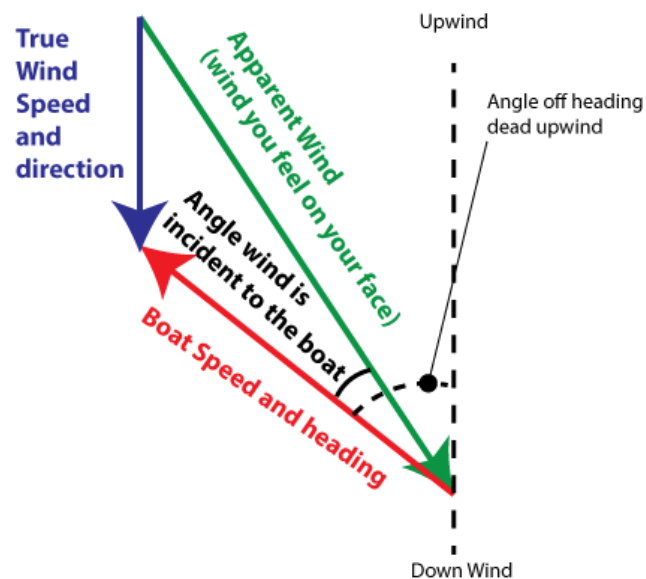


Figure 2 – Wind velocity triangle upwind (NauticEd, 2013)

2.1.2. Equilibrium Conditions

Once the wind is known, it is possible to derive the forces acting on a sailing vessel and balance them for a steady state sailing condition. For this, there must be an equilibrium between aerodynamic (sail) and hydrodynamic (hull) forces (Figure 3).

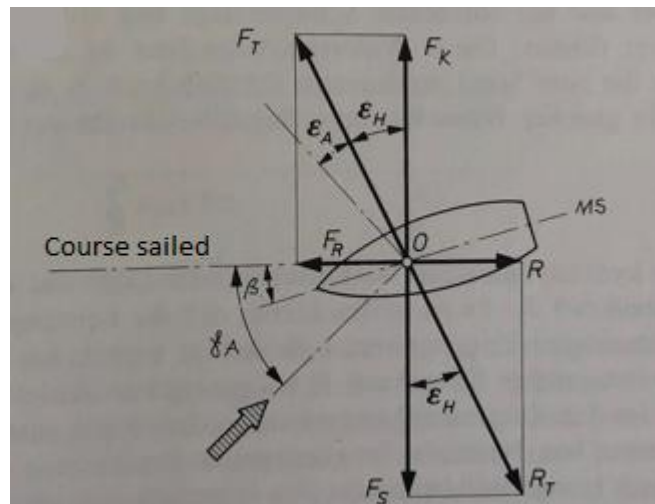


Figure 3 – Sailing forces equilibrium, adapted from (Marchaj, 1982)

The total aerodynamic force is composed by lift and drag, perpendicular and parallel to the incoming flow, respectively (Figure 4).

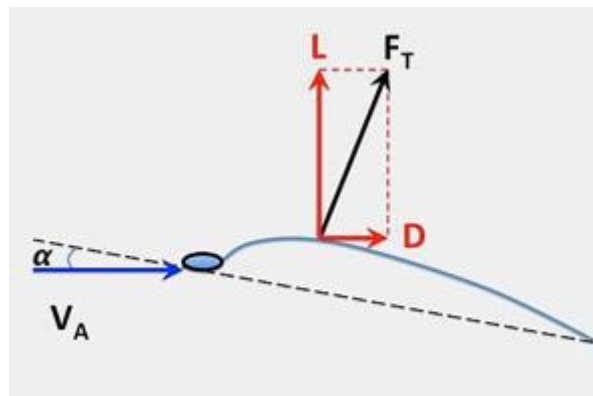


Figure 4 – Resultant aerodynamic forces (Fakiolas, 2020)

These forces arise from the pressure difference between sails leeward and windward sides when the sail is experiencing an apparent wind speed. They can be defined in function of apparent wind speed (V_A), sail area, air density and aerodynamic coefficients, as in equations 3 and 4:

$$L_A = \frac{1}{2} * \rho_{air} * V_A^2 * A * C_L \quad (3)$$

$$D_A = \frac{1}{2} * \rho_{air} * V_A^2 * A * C_D \quad (4)$$

Where C_L and C_D are, respectively, the coefficients of lift and drag, which depend on the sails angle of attack. Thus, the total aerodynamic force is the resultant from these two components (equation 5):

$$R_A = \sqrt{L_A^2 + D_A^2} \quad (5)$$

Moreover, the total aerodynamic force can be decomposed into two other ones: a driving force and a side force. The driving force acts along the course direction, thrusting the vessel forward to overcome the hydrodynamic resistance generated by the hull. The side force acts perpendicular to the course, producing a heeling moment and tilting the boat sideways, and is counterbalanced by the righting moment arising from hull, rudder and keel lateral forces (Figure 5).

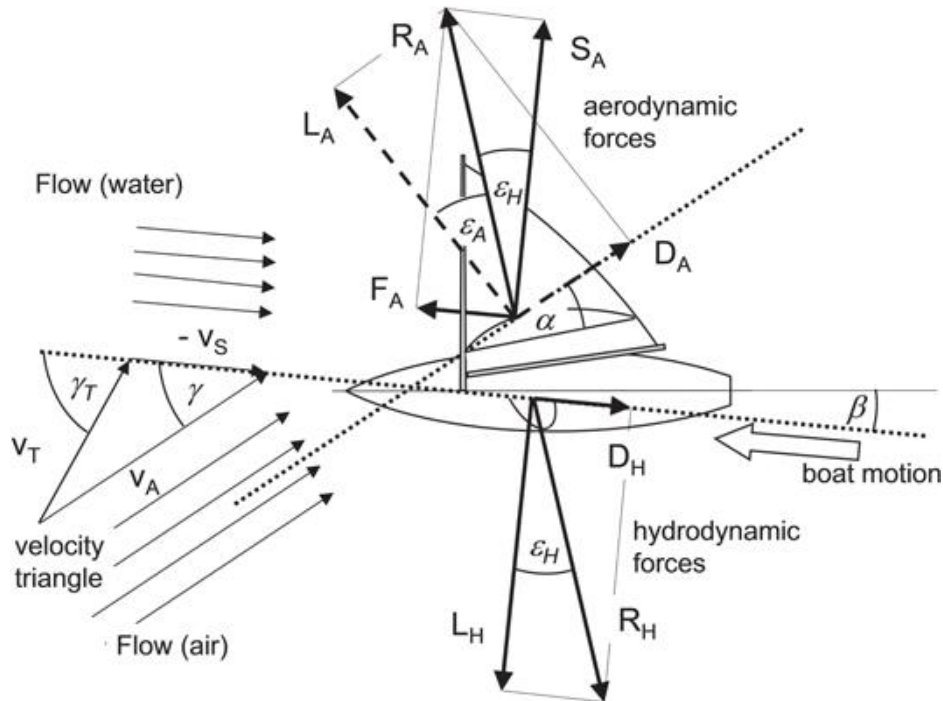


Figure 5 – Boat sailing steadily on the wind (Püschl, 2018)

Then, balancing both flow fields to have a stationary sailing condition (equations 6 and 7):

$$\vec{R}_A + \vec{R}_H = 0 \quad (6)$$

$$\vec{F}_A + \vec{S}_A + \vec{L}_H + \vec{D}_H = 0 \quad (7)$$

Where driving force (\vec{F}_A) and side force (\vec{S}_A) are expressed as in equations 8 and 9:

$$\vec{F}_A = \vec{L}_A * \sin(AWA) - \vec{D}_A * \cos(AWA) \quad (8)$$

$$\vec{S}_A = \vec{L}_A * \cos(AWA) + \vec{D}_A * \sin(AWA) \quad (9)$$

The predominant component in the driving force depends on the alignment of the sail with apparent wind. For smaller angles of attack, sails act as an aerofoil, enlarging lift participation and reducing the drag. On the opposite side, when sailing downwind, drag plays a major role. Sailing crafts utilize such knowledge to sail at high speeds even against the wind (tacking). However, ships with WAPS do not navigate in the same way as pure sailing vessels, not performing major alterations in their course to harness the wind. Therefore, it is not needed to go further into high performance systems since the presented theory regarding sails is already enough to understand how WAPS benefit from the wind.

The important point to be noted is the existence of different wind assisted propulsion systems, which present distinct aerodynamic coefficients (Figure 6). Some systems utilise predominantly lift component for generating the driving force, while others utilize drag one. It is, then, valuable, to take a closer look at them.

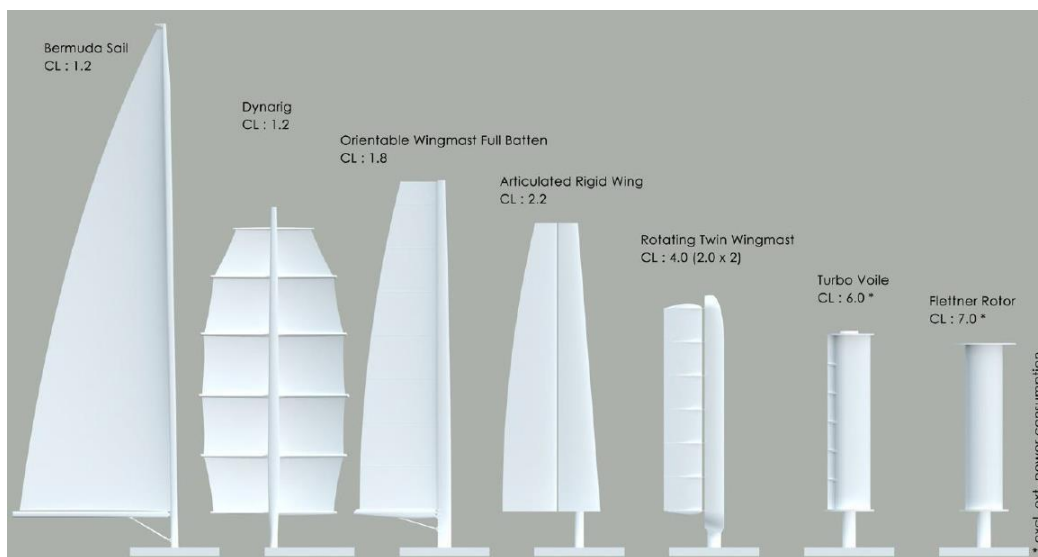


Figure 6 – Different sails and their lift coefficients (Mathis Ruhl Architecture Navale)

2.2. WAPS Overview

Now, there are systems already at use, as rotating sails, soft sails and ventilated foil systems, but many others are still under development or implementation, which is the case of kites, rigid wing sails and soft wing sails. Since the main purpose of the present thesis is not the performance of the systems, but a general procedure to assess the fatigue, a brief explanation about distinct WAPS is presented, without considering kites, as their attachment to the ship is considerably different from the other systems. The considered systems are, thus:

- Rotor sails
- Rigid wing sails
- Soft wing sails
- Soft sail systems
- Ventilated foil systems

2.2.1. Rotor Sails

Rotor sails, also called “Flettner rotors” after the German engineer and inventor Anton Flettner, are mechanically operated cylindrical sails whose rotation generates aerodynamics loads due to Magnus effect. In more details, the rotating cylinder accelerates the air flow on one side and decelerates on the opposite, resulting in a pressure difference that creates a lift force perpendicular to the wind flow direction. The longitudinal component of this force thrusts the ship (Figure 7).

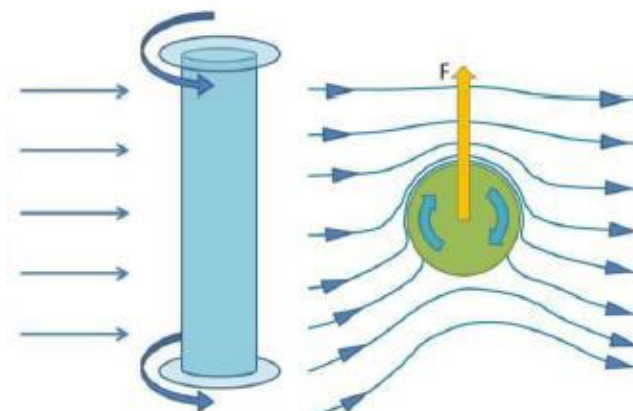


Figure 7 – Rotor sail thrust generation (Fakiolas, 2020)

The expected fuel savings vary from 4-5% for one sail, as in the case of the Scandlines's hybrid ferry M/V Copenhagen (Figure 8) (Norsepower, 2020), but can be even higher, especially if there are more rotors on deck. The tanker Timberwolf (previous Maersk Pelican), fitted with two Norsepower's rotor sails, presented confirmed fuel savings of 8.2% during the first year of operation (Norsepower, 2018). Pushing up to four rotors, ENERCON claims up to 25% reduction in fuel consumption when compared to same-sized freight vessels not fitted with the system (ENERCON, 2013).

Rotor sails present relatively small costs of installation and maintenance. Moreover, their lateral force can enhance manoeuvrability, and the characteristic of depowering themselves under high winds, reducing the aerodynamic loads, make them a hurricane proof device. However, the active rotation requires some power and generates vibrations, which should be taken with care.



Figure 8 – M/V Copenhagen (Norsepower, 2020)

2.2.2. Rigid Wing Sails

Rigid wing sails are formed by aerofoil sections that, different from airplane wings, can generate lift on either side. They can rotate and, so, are able to utilize different incoming wind angles relative to the ship direction. In this sense, the system is designed to operate at an optimal angle of attack relative to the apparent wind direction, providing the maximum lift coefficient with the smaller possible drag coefficient (Fakiolas, 2020). Moreover, the geometry of rigid wing sails provides higher lift-to-drag ratio than traditional soft sails (Reche, 2020).

Besides, they are also easy to be operated and trimmed for wind conditions due to their internal structure. The system can also be retractable, reducing risks at storms and for cargo

handling (Reche, 2020). Due to its potential benefits, there are some projects in the area, as one from Windship Technology (Figure 9).



Figure 9 – Windship Technology rigid wing sails (Ovcina, 2021)

2.2.3. Soft Wing Sails

These wind propulsors are similar to the rigid wing sails, but they have a softer coverage surface material. This makes reefing procedure easier. When the wind becomes unfavourable, the wing sail is reefed and furled instead of retracting.

One example of such applications is the project of Oceanwings (Figure 10), by Ayro, already implemented a full-scale prototype in a catamaran (Figure 11). Another idea that could fall into this category is the inflatable Wing Sail Mobility (WISAMO), by Michelin (Figure 12) (Michelin, 2021).



Figure 10 – Oceanwings (Ayro, 2021)



Figure 11 – Oceanwings installed in prototype (Ayro, 2021)



Figure 12 – WISAMO inflatable sails (Michelin, 2021)

2.2.4. Soft Sail Systems - DynaRig

DynaRig is a square rig developed in the late 1960's, characterized as a free-standing mast with curved yards rigidly attached to it. The soft sails are deployed on these yards in order to present no gaps between them, creating a single panel to capture the wind. They are about twice as efficient as traditional square rig sails and can maintain much higher average sailing speeds (Reche, 2020) (Fakiolas, 2020).

Such systems were already applied to yachts, as Maltese Falcon (Figure 13) and Black Pearl, but are still a concept for commercial vessels, as in the case for WASP Ecoliner (Figure 14) developed by Dykstra Naval Architects (Dykstra, n.d.).



Figure 13 – Maltese Falcon (Maltese Falcon, 2020)



Figure 14 – WASP Ecoliner (Dykstra, n.d.)

2.2.5. Ventilated Foil Systems

These systems are named as “foils”, but actually they present a large thickness compared to a typical aerofoil and a relatively small chord-length, resulting in an egg-shaped cross section. At the leading edge, the airflow is accelerated, resulting in a low pressure zone in one side.

This zone can be “elongated” with the installation of a ventilator to control the airflow around the thick foil-shape, applying a boundary layer suction.

The suction prevents the separation of the flow while maintaining the advantages of high-pressure differential developed by the thick shape. It is an artificial way to reduce the drag coefficient of the wing profile while keeping the lift coefficient high. The direction of the leading edge is adjusted to an optimal angle of attack to the apparent wind.

The ventilated foils are already available in different sizes and aspect ratios depending on the design of the system. They are even already installed in small multipurpose ships, as the Ventifoils (Figure 15) from eConowind (eConowind, 2021). This system is fully automated and can be folded in case unfavourable wind conditions or during cargo operations.



Figure 15 – Retrofitted Ventifoils installed (eConowind)

2.3. Fatigue for WAPS

Research on wind assisted propulsion systems has been focused, so far, on the performance and economic advantages of these systems (Reche, 2020) (Bordogna, 2020). Since they are still being developed and implemented, it is necessary to justify their gains for supporting their adoption in larger scales. More than that, it is also important to explore possibilities and understand better how to enhance those gains.

And if they are to be installed, then the first step is to assure the integrity of the WAPS. This can be done for extreme loads and worst-case scenarios, providing a robust design against this type of loads for a new built system. Extreme loads are relatively simple to be estimated by present rules and standards, especially if adopting a conservative approach.

But fatigue analysis is also necessary to assure that the appliance will endure repeated efforts along its lifetime. In this sense, since fatigue is mostly affected by regular loads, conservatism regarding them is not so desirable, avoiding a too robust design. And there should be a good understanding of the loads acting on WAPS.

This problem could be dealt in an individual basis so far, due to the limited number of WAPS in operation. The most important for the new systems was, until now, to prove that they could withstand extreme loads. However, with the ageing of those systems and the increase in their adoption, it would not be practical to keep the same approach for fatigue analysis.

There are already some standards to guide the design of WAPS and, therefore, before any modification proposal, they should be reviewed in order to understand their assumptions, applicability and limitations. Knowledge from similar areas may also help to enhance these standards, adding a broader view on the fatigue problem. By last, it is also important to verify which effects and loads are important and which can be neglected.

2.3.1. Rules and Limitations

By the moment this thesis began to be developed, standards for WAPS could be found in (DNVGL-ST-0511, 2019) “Wind assisted Propulsion Systems” (from November 2019, with corrections from March 2021), which could be used for the purpose of certification. Such standard was developed for a group of WAPS: rotor sails, soft wing sails, soft sail systems and ventilated foil systems (Figure 16). The technical requirements in this are generic enough so that it could be applied also for other types of WAPS in close association (DNV-GL, 2020).



Figure 16 – WAPS approached by DNVGL-ST-0511 (DNV-GL, 2020)

The standard is, however, economical in the way it describes the necessary fatigue assessment. It gives a brief recommendation regarding vibrations, orientating that a vibration analysis shall be carried out in case the WAPS is exposed to vibrations. For fatigue strength, it states that the calculations shall be carried out in accordance with (DNV-RU-SHIP Pt.3 Ch.9, 2021).

Such rules provide approach only for typical ship structures, while WAPS are not so common (so far). Therefore, it was suggested to apply (DNVGL-ST-0377, 2018), a Standard for Shipboard lifting appliances. This has been developed for shipboard cranes, similar to WAPS in the way they are disposed on deck and exposed to weather conditions.

In this standard, there are two modes of operation, “in operation” and “out of operation”. For a WAPS, this definition should be reversed since they operate in windy conditions for the navigating ship, while cranes try to avoid any excessive wind during operation for the stationary vessel. Therefore, what is described as “out of operation” for cranes describes the scenarios at sea for WAPS.

These modes of operation could be applied for the present standard, which considers that WAPS are exposed to two main characteristic fatigue loadings: inertia and wind loads. The first consider the effects emerging from the self-weight and dynamic forces on WAPS excited due to ship motions. The second are converted to thrust forces and, thus, are very important during their operation, but may also be considered when in condition “out of operation” (for WAPS) since the system may be still exposed to wind loads even so.

The characterization of inertia fatigue loads can be obtained from a maximum stress range, an assumed number of cycles during an expected lifetime and the probability distribution. This relation is described by stress range spectrum A (DNVGL-ST-0377, 2018), where the stress range values are a fraction of the maximum stress range (Figure 17).

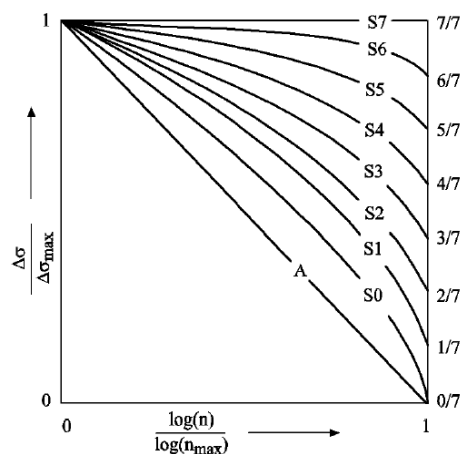


Figure 17 – Fatigue stress spectra (DNVGL-ST-0377, 2018)

The accelerations determined from envelope accelerations, taken from (DNV-RU-SHIP Pt.3 Ch.4, 2021) Sec.3 [3.3.4], and serve to determine the maximum design loads for the structural assessments.

The wind load acting on WAPS, shall be calculated from the apparent wind speed, including the effects of gusts, considering pertinent aerodynamic coefficients (lift and drag) and air flow conversions from technical evidence. In this sense, the characterization of wind fatigue loads may be derived using a wind energy spectrum, as the “Frøya Energy Spectrum”, from (DNV-RP-C205, 2019) Sec.2 [2.3.4.12], allowing the generation of a variable amplitude history for a given mean wind speed at a given height (parameters necessary for the wind spectrum). However, the shape of the stress spectrum for wind loads would present more cycles in the lower stress ranges as wind variations are not so large but occur at higher frequencies.

The main problem, though, is how to combine both loads. One single stress range spectrum may be chosen, but this would not be strictly correct since loads are not in phase. Nevertheless, considering maximum loads acting at the same time would be conservative. Another simplification in this sense is to consider the same number of cycles for wind and wave oscillations, easing the sum of their resulting stress spectra.

However, other problems arise from this point. Wind and waves may not be aligned and present different correlation regarding their magnitude. This is an issue not only for WAPS, but also for other systems at sea.

2.3.2. Offshore Wind Turbines Experience

Therefore, it is suggested to look at similar areas in the maritime industry to understand how they deal with such problems. This is the case for offshore wind turbines, for example, which can be fixed or floating (moored) systems and for which the fluctuating wind and wave loading are also the most significant loads needed to be considered when performing the fatigue assessment. For these, the dynamic response is more significant than that of traditional platforms used in the offshore petroleum industry due to the wind loads effect (Yeter, Garbatov, & Guedes Soares, 2013).

The random nature of the environmental loads in terms of amplitude, position and direction means that wind turbine supporting structures are subjected to a great variety of stress ranges, with the predominant loads varying according to the environmental state. However, wind loading presents non-linear behaviour, which makes it difficult to analyse these loads in the frequency domain (wave loads can be linearized, wind loads not). The current design practice,

therefore, is to utilize prescribed time domain simulations with complete turbine dynamics and control and simultaneous wind and wave loading (Yeter, Garbatov, & Guedes Soares, 2013).

Although presenting good results, such procedures are time demanding. To simplify the assessment for such cases, joint probability methods developed to simulate the occurrence frequencies of environmental loads may be combined with a transfer function for wind and wave loads, but this process depends on the location and on the floating system configuration (Yeter, Garbatov, & Guedes Soares, 2013). At this point, WAPS differ from such systems since they can be applied for different ships in a global range.

However, even for wind turbines, the approach is not definitive. For example, a coupled analysis method can be utilized based on the assumption that the phasing of wind and wave loads is stochastic and correlated (Yeter, Garbatov, & Guedes Soares, 2013), but, if the phasing of wind and wave load is regarded as non-correlated (Dong, Moan, & Gao, 2011), then a decoupled analysis may be applied. In other points, they agree though, as relying in the time domain assessment and considering wind turbulence intensity as 0.15 (Yeter, Garbatov, & Guedes Soares, 2013) (Dong, Moan, & Gao, 2011).

Moreover, other very important aspect is the direction of waves and wind, or, more specifically, their alignment. The wind-wave misalignment affects the motion and the structural load of wind turbines (Li, Zhu, Fan, Chen, & Jianjun Tan, 2020). Such effects are also of interest for WAPS, especially if considering that the ship forward speed adds another misalignment factor between the loads.

It is known that wind and waves spread out in all directions and that their misalignment is measured as the temporal difference between the wind direction and mean wave directions. Regarding this aspect, highest degree of misalignments is found at low wind speeds, and minor misalignments are found at high wind speeds. Moreover, most misalignment occurs up to 30° , with frequency being less than 5% for wind-wave misalignment greater than 60° (Verma, Jiang, Ren, & Gao, 2020).

This is even more complicated considering that wave and winds also vary in terms of magnitude. It is true that significant wave height depends on the wind speed, but it should be considered that not only locally generated waves encounter the ship and swells also need to be accounted for. Swells result from distant storms that travel a significant distance and arrive often at an angle that differs from the wind direction, presenting, so, differences in the magnitude and directional correlations.

In fact, the consideration that significant wave height and period are a function of the wind speed is based on the fully developed sea assumption. It considers that waves come into equilibrium with the wind that blows with a steady speed and direction over a long period of time and large area (Benitz, Lackner, & Schmidt, 2015) (Marghany, 2020). This is, however, not true, but simplifications can be used in this sense (Benitz, Lackner, & Schmidt, 2015).

Regarding these simplifications, they can be applied with some conservatism, considering the sea states as a function of the wind speed, and representing the direction of the waves by its misalignment relative to the wind. In this sense, wave climate is considered under the wind probabilities, what may not accurately reflect the real conditions of the site and consequently, wave fatigue damage may be misrepresented (the opposite, i.e. representing wind directions based on waves, can also be done, but the problem would just be transferred for the other weather condition). Since the other option is to run many lengthy simulations, some assumptions are made to support the application of the simplifications, as limiting the number of wind and wave combinations to be analysed using suitable wind/wave relationships based on their natural correlation (Hodgson, Sampathkumar, & Cortizo, 2016).

Normally, one sea state is defined for per direction each wind speed. Regarding the directions, sometimes only one is considered for all environmental states (Yeter, Garbatov, & Guedes Soares, 2013) (Dong, Moan, & Gao, 2011), but a more careful analysis should, at least, consider a reduced number of misalignments at lower wind speeds. At high wind speeds, wind and wave directions are found to be predominantly aligned and, therefore, little or no misalignment needs to be considered (Hodgson, Sampathkumar, & Cortizo, 2016).

2.3.3. Other Factors

Further aspects should be considered for WAPS, especially because ships differentiate from platforms (fixed or moored) in a fundamental point: ships navigate. This adds or, at least, enhances some effects as ship motions and vibrations. Vessels are more subject to oscillate due to environmental loads and more vibration sources appear.

Inertia loads

Regarding ship motions, ships are normally studied in a 6 degrees-of-freedom system, represented by translations along and rotations around a vertical axis, a longitudinal axis and a transverse axis.

The motions and their sign convention are defined as in (DNV-RU-SHIP Pt.3 Ch.4, 2021) and can be seen in (Figure 18):

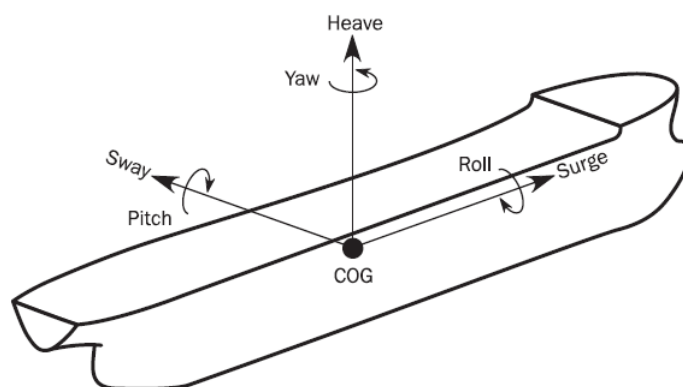


Figure 18 – Definition of ship motions (DNV-RU-SHIP Pt.3 Ch.4, 2021)

- positive surge is translation in the X-axis direction (positive forward)
- positive sway is translation in the Y-axis direction (positive towards port side of ship)
- positive heave is translation in the Z-axis direction (positive upwards)
- positive roll motion is positive rotation about a longitudinal axis through the COG (starboard down and port up)
- positive pitch motion is positive rotation about a transverse axis through the COG (bow down and stern up)
- positive yaw motion is positive rotation about a vertical axis through the COG (bow moving to port and stern to starboard).

The inertia loads are important for the fatigue assessment, as previously noted, but not necessarily in all degrees of freedom. Regarding the WAPS, the main inertia effects arising from ship motions are caused by roll, sway and heave, what means longitudinal, transverse and vertical accelerations. These will generate stress loads on the equipment and, therefore, needed to be approached by envelope accelerations, for example.

Vibrations

The operation of the ship in waves also induce vibrations of the hull girder. Vibrations, in general, may be a large problem if the WAPS natural frequency matches one of the excitement frequencies of the ship, of the engine or the propeller. However, to predict the excitement frequencies is not so trivial and these are measured during sea trials.

Anyway, it is possible to avoid some common values for ship excitement frequencies, as 0.5Hz for the hull girder. And, in case one of these matches the equipment natural frequency,

the problem is normally easy to be detected due to excessive vibration of the structure. It may be solved by adjusting the system or attachment stiffness or even damping the support to avoid the critical frequencies.

Vibrations may also arise from the WAPS itself or as a result from the wind acting on them. Imbalanced rotor sails, for example, may vibrate, but this should be solved by simply balancing the system. Those systems, since they are slender, would also be most susceptible to vortex induced vibrations due to wind, but their slenderness can be adjusted in this sense.

Wind induced by ship motions

Wind also presents different interactions with the ship. The most obvious one, approached when studying the physics for sailing, is the apparent wind speed from the combination of ship and true wind speeds. This aspect is fundamental for assessing the wind loads on WAPS and must be always considered.

Moreover, there are also other ship motions besides forward one, especially pitch and roll. The amplitude of those motions is, however, not large and the effects are already accounted for inertia loads. The wind induced by such motions would not be dominant, except for extreme rolling or pitching situations, when the WAPS would not be utilized for safety reasons, therefore they are not considered in further analyses.

Still regarding the interactions, the vessel itself affects the wind passing around the hull. The freeboard and superstructures may affect the performance of the WAPS, and, thus, this problem should be approached by the designer. Such effects are also not considered, assuming wind blockages are avoided or, at least, that they present low impact.

In the opposite sense, there also effects from the WAPS in the ship, as damping the motions, heeling or affecting course keeping. These can present benefits or losses in a small scale for most cases (Fakiolas, 2020). However, these are not the focus on the present thesis and are regarded to have low impact on the whole operation, being, thus, not relevant for fatigue loads

Wind

Still regarding wind, it is important to consider its different variations, as wind can vary according to the spatial coordinates and present speed fluctuations along the time. Moreover, speed also changes in direction and speed along the height, presenting a speed profile.

Therefore, it is fundamental to establish consistent ways to assess the wind speed, retrieving it always for the relevant height.

This impacts directly on the wind loads assessment since aerodynamical coefficients depends on the wind alignment in relation to the WAPS and wind speed greatly affects the loads on sails. Such aspects, especially the wind speed profile, must be, thus, always included in the analysis for wind forces, either it is for fatigue calculation, extreme loads or vessel speed performance.

WAPS operation

From the perspective of the WAPS itself, the operational profile and control systems shall be taken into consideration. The dynamic loads will be driven and limited by the configuration and operation of the system. This aspect can vary considerably among different WAPS, but, at the same time, it needs to be approached in a general way to ease the assessment of regular and maximum operational loads.

From the operational point of view, the utilization of WAPS would suit weather conditions for which the wind comes at certain directions with enough speed to thrust the vessel. As stated, such situations are different according to each system, but the important aspect here is that the system should be able to generate a higher thrust for the vessel than the resistance force it creates. In this sense, for winds that are “weak” or coming from unfavourable directions, the system can be furled or even aligned to the wind in such a way it presents lower resistance (or no resistance at all in the case it can be fully retracted and “hidden”).

On the other extreme, there are strong winds or severe weather. For performance, strong winds would be favourable, depending on their alignment with the ship. However, very strong winds may be able to generate too high loads for the system, what may be dangerous. Therefore, there is also a limit on the upper side, for which systems can operate in maximum capacity without risking their structural integrity.

Naturally, during very severe weather it is risky to utilize such systems due to the high loads imposed to the sails (not only by wind, but also for severe rolling situations, for example). For these extreme situations, the WAPS may also be furled to avoid them or minimize their effects. If there are strong winds only, it is possible to align the sails relative to the wind or let them vane with it, what would allow to depower the sails or minimize lift and drag without retracting and stowing the system for every risky situation.

Still in this sense, it is better to keep the system operating at its maximum performance for a range of wind speeds and directions (not only for one ideal situation). This means that, for weak or moderate winds, the idea is to extract the maximum power as possible, by maximizing the camber (and the lift) for example. On the opposite way, operating at range of higher wind speeds means that the system should be able to limit the loads (depowering), what can be achieved by reefing the sail, adjusting the camber or its alignment, depending on the WAPS.

It means that situations for the utilization or not of the WAPS need to be defined for each system. Not only this, but also how the WAPS should operate for each situation. This directly affects the performance of the system and the possible damages to it, as the operational profile determines the time and level of exposure of the system to the loads (or whether it is not exposed at all).

WAPS interaction

The WAPS presence not only affects the air flow regarding the ship, but also the incoming air to other WAPS, if there is more than one equipment installed. For rotor sails located to close one to the other, for example, the performance may decrease as the drag increases (Bordogna, 2020) (Fakiolas, 2020). However, this should be considered by the designer and, therefore, the thesis will consider that incoming wind is not disturbed by other structures.

3. FATIGUE

During the design of a ship, different limit states are considered regarding the structural resistance. There are normally four of them: serviceability, ultimate limit states, fatigue limit, accidental and fatigue limit states. Among these, fatigue is a significant failure mode of ships and, therefore, associated failures must be avoided or at least controlled to exclude costly repairs and catastrophic events (Fricke W., 2017).

Fatigue generally occurs in conjunction with fluctuating (cyclic) loads and hence, stresses (Figure 19 and Figure 20), which can be subdivided according to their frequency and/or period. Such load variations may arise from loading conditions, ship motions in the seaway (combined with the weather), engines, propellers, hull vibrations, etc. In general, it can be assumed that all structural members subjected to high cyclic stresses are prone to fatigue.

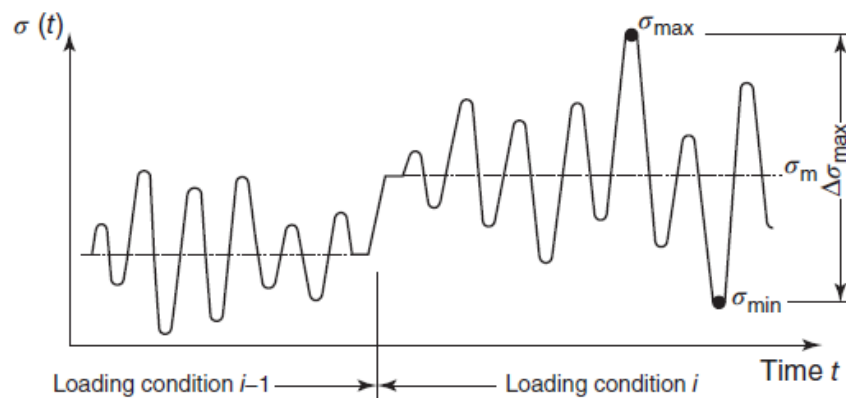


Figure 19 – Stress history (schematic) (Fricke W., 2017)

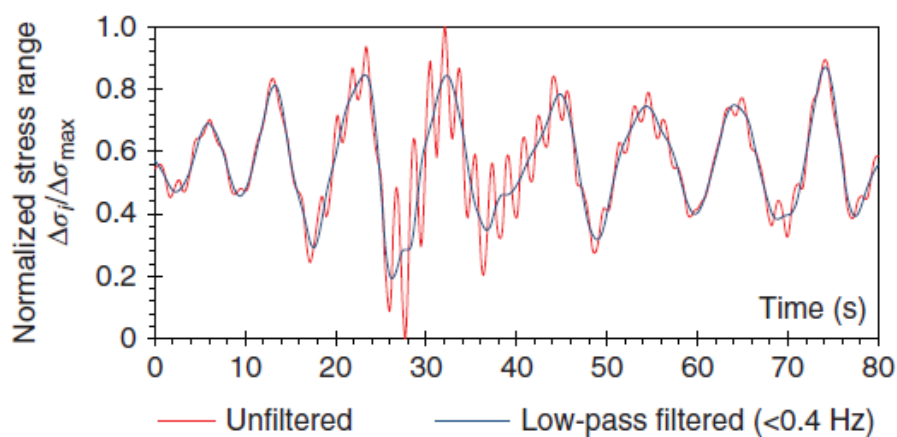


Figure 20 – Stress history from on-board measurement (Fricke W., 2017)

Thus, the fatigue strength of a structure is mainly influenced by the severity of the loading (the number and amplitude or range of stress cycles) and characterized by the amount of the stress concentration and mean stress. In this sense, although they have different origins, the induced loads must be superimposed to calculate the maximum and minimum stresses, σ , and the respective stress ranges, $\Delta\sigma$, which will result in the stress range spectrum (Fricke W., 2017).

Therefore, fatigue tends to occur in stress concentration areas. But a crack initiation site is also affected by other factors as: material properties, residual stresses, corrosion, and misalignments. Thus, it is important not only to minimize such problems, but also to monitor and control the fatigue damage along the ship lifetime, keeping it within acceptable limits.

However, the inspection of all possible crack initiation sites may not be possible, or the cracks may propagate unexpectedly too fast. In this sense, there are guidelines that allow one to estimate the fatigue damage for a ship along its lifetime. These require the consideration of diverse loads and effects according to the location evaluated.

For wind assisted propulsion systems this is not different, but, before anything in that point, it is important to understand the principles that dominate the fatigue damage assessment. It is, then, fundamental to approach how stresses are assessed and how the cyclic loads contribute to the total fatigue damage of the WAPS foundation. The stress overview is done in the context of loads caused by waves, well covered by the rules, applied for steel.

3.1. Fatigue Approaches and Stress Assessment

Fatigue assessment may be performed for nominal stresses, or local stresses at free plate edge, hot spot stresses, or weld-notch stresses, being this last one not so frequently used. Nominal stress neglects stress raisers due to the structural geometry and local notches. Hot spot and notch stresses include the stress increase due to the structural geometry, but the first neglects the effects due to local notches at weld toes, while the second also includes this.

The S-N curve applied for assessing the fatigue life depends directly on the type of stress adopted. The fatigue life is calculated with basis on nominal stress S-N curves in the first case. Hot spot stress S-N curves are utilized, as their name suggest, for hot spot stresses, which can be calculated from direct calculations or through the application of tabulated stress concentration factors (K).

Nominal stresses consider the stress as undisturbed by notches like cut-outs or welds. They are derived by beam theory, that is, they can be defined by integral load parameters and

sectional properties. This is the approach for beam models or coarse finite element models. However, applying K factors is necessary in this last case if the FE model neglects stress concentration effects due to geometry (Fricke W., 2017).

For nominal stress approaches there are different design S-N curves according to the structural detail, that give the fatigue strength of same or similar details subjected to a well-defined nominal stress. Typical imperfections such as misalignment are already included in the fatigue classes as these were present in the underlying fatigue tests (Fricke W., 2017).

Hot spot stresses also consider the stress increase caused by structural discontinuities and presence of attachments, being applied to shell element FE models. The local stress increase due to the weld toe is, however, excluded. The hot spot S-N curves already accounts for stresses arising from the local weld geometry, excluding such effects from the stress calculation. In contrast, if the effects of the structural geometry are already considered in the structural stress, a single S-N curve is sufficient for each type of weld and material (Fricke W., 2017).

However, once again, a single stress is not the relevant point for fatigue analysis. Fatigue loading is based on the long-term stress range distribution, allowing this loading to be compared to S-N curves, which represents the fatigue capacity. For a ship in waves, the stress range may be calculated by formulations prescribed by rules, by ship specific design wave loading or based on directly calculated hydrodynamic loads, considering specific ship and specific wave scatter diagram.

The level of detailing and complexity from prescriptive to direct methods varies significantly. Naturally, a refined design analysis improves the reliability of the calculated fatigue life, but generally prescriptive methods for fatigue assessment already give a good representation of the fatigue strength. The choice will depend on the structural details, the consequences of the damage and experience with the methods for similar situations.

3.2. Fatigue Stress Range

The relevant parameters for the fatigue damage process, that is, stress range $\Delta\sigma$ of the individual cycles and mean stress σ_m , can be derived from a measured or simulated history by different cycle-counting methods. The rainflow method is preferred as it considers the related elastic-plastic material behaviour causing the fatigue damage (Fricke W., 2017).

The fatigue stress range, $\Delta\sigma_{FS}$, in MPa to be used in the assessment is based on the calculated stress range, $\Delta\sigma$. However, before performing fatigue strength assessment, the calculated stress entered in the S-N curve needs to be corrected for several correction factors (equation 10).

$$\Delta\sigma_{FS} = f_{mean} \cdot f_{thick} \cdot f_{material} \cdot f_w \cdot f_c \cdot f_s \cdot K_m \cdot \Delta\sigma \quad (10)$$

The calculated stress range is estimated as:

- From beam model (equation 11):

$$\Delta\sigma = |\sigma_2 - \sigma_1| \quad (11)$$

- From FE model for standard details, according to (DNVGL-CG-0129, 2019) Sec.6 [4]: (equation 12):

$$\Delta\sigma = |\sigma_2 - \sigma_1| * 1.12 \quad (12)$$

- For web stiffened cruciform joint, according to (DNVGL-CG-0129, 2019) Sec.6 [5] (equation 13):

$$\Delta\sigma = |\sigma_{2,shift} - \sigma_{1,shift}| * 1.12 \quad (13)$$

- From FE model for simplified cruciform joint, according to (DNVGL-CG-0129, 2019) Sec.6 [6] (equation 14):

$$\Delta\sigma = K/K_m * |\sigma_2 - \sigma_1| * 1.12 \quad (14)$$

Where:

σ_2 = stress from mean wind plus gust, or crest phase for inertia

σ_1 = stress from mean wind minus gust, or through phase for inertia

As mentioned, different factors and considerations may apply for the stress to be entered in the S-N curves.

3.2.1. Scantling Approach Factor, f_c

Finite elements models may be based on either net scantling, t_{n50} , or gross scantling, t_{gr} . However, for prescriptive fatigue assessment, the calculated stress range should follow the net scantling approach, t_{n50} . Moreover, the scantling approach factor, f_c , shall be applied.

When the FE model of the foundation is based on gross scantlings, the f_c factor shall be taken as 1.0. Gross scantlings without any deduction for corrosion addition shall be applied for beam models, also considering f_c as 1.0 from (DNVGL-CG-0129, 2019) Sec.3 [2.2]. No corrosion can be assumed since the steel foundation of the WAPS is considered above the deck (DNV-RU-SHIP Pt.3 Ch.9, 2021) Sec.4 [4.4].

3.2.2. Environmental Factor, f_e

From (DNV-RU-SHIP Pt.3 Ch.9, 2021) Sec.4 [4.2], the f_e factor may be taken as 0.8 for worldwide operation or as 1.0 for North Atlantic. To contemplate operation in different areas, the factor for worldwide operation shall be applied ($f_e = 0.8$). In case of direct hydrodynamic calculations based on a specific scatter diagram, for a specific route, the f_e factor is set to 1.0 or omitted (DNVGL-CG-0129, 2019) Sec. 3 [2.3].

3.2.3. Mean Stress Factor, f_{mean}

For fatigue analysis the stress range may be reduced dependent on whether the cycling stress is in tension or in compression (DNVGL-CG-0129, 2019) Sec. 2 [4]. The stress range may be reduced if part of the stress cycle is in compression. Therefore, for a conservative approach, assuming that the material is in tension during the entire stress cycle, mean stress factor $f_{mean} = 1.0$ shall be applied.

3.2.4. Thickness Effect, f_{thick}

The fatigue strength of welded joints is also affected the plate thickness. This effect occurs due to the local geometry of the weld toe in relation to thickness of the adjoining plates. It is also dependent the stress gradient over the thickness (DNVGL-CG-0129, 2019) Sec. 2 [5].

For steel plates with thickness less than 25 mm, the correction factor, f_{thick} , is taken as 1.0. For thicker plates, the factor depends on the effective thickness and on the detail evaluated. More details for this case can be found in (DNVGL-CG-0129, 2019) Sec. 2 [5].

3.2.5. Material Factor, f_{material}

The material factor, f_{material} , shall be taken as 1.0 for normal steel and welded details. For higher tensile steels, the fatigue stress range should include a correction factor for the material strength, according to (DNVGL-CG-0129, 2019) Sec.2 [6].

3.2.6. Post Weld Treatment Factor, f_w

There are limitations for the benefit of post-weld treatment. Therefore, this factor, f_w , should preferably not be considered in the initial design phase and shall be applied as 1.0. However, in case of weld profiling and toe grinding, post weld treatment may be accepted on a case-by-case basis

3.2.7. Misalignment Factor, K_m

For beam models, the tabulated stress concentration factor (K) may already include standard misalignment. However, it also may not be included in this case or for finite element analysis. Therefore, an additional misalignment effect shall be included for simplified cruciform joints, as dealt in (DNVGL-CG-0129, 2019) Sec.6 [6].

Such effect may arise from the variation of the loads on each side of the mast, with a bending leading to compression on one side and tension on the other. Then, for a highly utilized deck, the mast pedestal may not be continuing through deck to the foundation below deck. Eccentricities also play a role at this effect and, thus, should be controlled during construction.

3.2.8. Stress Range Spectrum

The stress range can be represented in terms of a stress range spectrum. This can be done for the appliance itself or for details, considering working loads or stress ranges, respectively. In any case, the stress range spectrum describes the frequency of the different working loads (for an appliance) or stress ranges (for a detail) to be expected during the lifetime of the appliance. It is also important to notice that, regarding the fatigue strength analysis, it shall be taken into consideration that the standard stress range spectrum of appliances and the stress range spectrum of a design detail may be different in terms of form of spectrum and in terms of number of load cycles or stress cycles, respectively (DNVGL-CG-0129, 2019) Sec.3 [2.1]. The evaluation of long-term stress measurements from fatigue analyses has resulted in typical frequency distributions of stress ranges due to the seaway which are usually represented as cumulative distributions of stress ranges (also designated as stress range spectra). These can frequently be approximated by two-parameter Weibull distributions, as in equations 15 and 16 (Fricke W., 2017).

$$Q(\Delta\sigma) = \exp\left[-\left(\frac{\Delta\sigma}{q}\right)^\xi\right] \quad (15)$$

$$q = \frac{\Delta\sigma_0}{(\ln n_0)^{1/\xi}} \quad (16)$$

where:

Q = probability of exceeding the stress range $\Delta\sigma$

ξ = Weibull slope parameter

q = Weibull scale parameter.

The stress range distribution may also be expressed as in equation 17:

$$\Delta\sigma = \Delta\sigma_0 \left[\frac{\ln n}{\ln n_0} \right]^{1/\xi} \quad (17)$$

where:

$\Delta\sigma_0$ = reference stress range value at the local detail exceeded once out of n_0 cycles

n_0 = total number of cycles associated with the stress range level $\Delta\sigma_0$.

The Weibull slope depends on the location of the detail and the governing load components. The reference level for the stress is not significant if the Weibull slope and scale parameters are well established. Alternatively, the fatigue strength may be assessed by considering the different encountered sea states and summarizing the short-term results from all the sea states (DNVGL-CG-0129, 2019) Section 3, [2.1].

Several long-term measurements of wave-induced stresses have shown that the shape parameter is close to unity which results in the so-called straight-line spectrum in a linear-logarithmic representation. Such standardized distributions are usually assumed during fatigue design, where the parameters, that is, the characteristic stress range and number of stress cycles, are either directly computed or based on the assumptions given in the rules of the classification societies (Fricke W., 2017).

For the sails, the stress range spectrums utilized as basis are taken from (DNVGL-ST-0377, 2018) [4.6.5], rules for lifting appliances (Figure 21). For these, regarding the fatigue strength analysis for the condition in-operation, normally it is possible to categorize the lifting appliances in groups corresponding to the standard stress range spectra S0 to S7. For the condition "out of operation", the fatigue strength analysis shall be conducted for the straight-line spectrum A according to a total number of stress cycles $n_{\max} = 5 \cdot 10^7$.

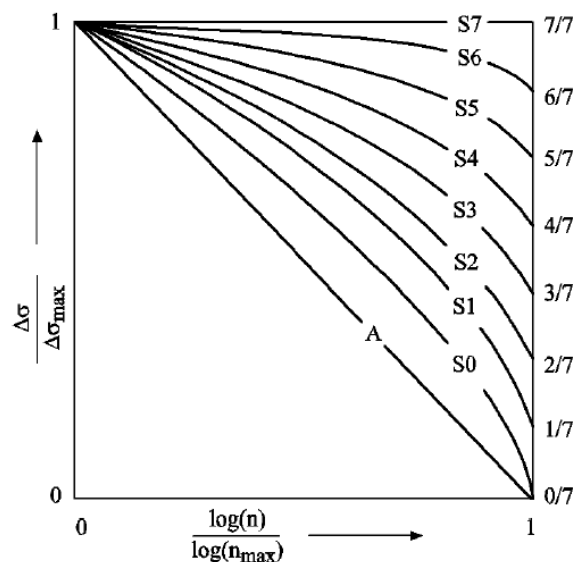


Figure 21 – Standard stress range spectra (DNVGL-ST-0377, 2018) [4.6.5]

However, lifting appliances and WAPS differ in their operational profile: the first is utilized while the ship is at port, but WAPS are utilized during navigation. This inversion in the operation leads to the utilization of the curve A for WAPS under sea loads. Moreover, the

number of stress cycles is also modified to account for the operational time at sea for this equipment.

It is important to remember that WAPS are also subjected to wind loads. For this, a stress range spectrum should be developed for each system, according to their sail area and aerodynamic coefficients. At some point, it should present a threshold, when control systems act to avoid overloading, represented by the S7 spectrum.

Naturally, if the operating conditions are exactly known, individually determined stress range spectra may be used for the fatigue strength analysis, based on calculated cumulative damage ratios. In this case, the individual stress range spectra shall be proven by the manufacturer (DNVGL-ST-0377, 2018) [4.6.5].

3.3. Fatigue Strength Assessment

In ship structural design, the S-N approach is applied in most cases for assessing the fatigue strength of structures. This approach requires using appropriate S-N curves either directly in the case of constant amplitude loading or in conjunction with a damage accumulation hypothesis in the case of variable amplitude loading.

In the latter case, when there is a complex loading, rainflow can be utilized for creating a histogram of simple cyclic loadings. The rainflow cycle counting method was introduced in 1968 by Matsuishi and Endo and named from a comparison of this method to the flow of rain falling on a pagoda and running down the edges of the roofs. This method identifies hysteresis loops within a load, stress, or strain time history (Lee & Tjhung, 2012).

Then, for each stress level, it is possible to calculate the respective damage according to the correspondent S-N curve. The last step is to combine the individual damage contributions from each stress range through Palmgren-Miner rule for damage accumulation (Fricke W., 2017).

3.3.1. S-N Curves

One of the basic elements for the S-N approach is the S-N curve itself. Obtained from fatigue tests, S-N curves represent the fatigue capacity of welded joints and base material. They are based on the mean-minus-two-standard-deviation curves, which are associated with a 97.5%

probability of survival (DNVGL-CG-0129, 2019). Moreover, usually unfavourable mean and residual stresses are assumed (Fricke W., 2017).

Different S-N curves may be applied according to welded details and base materials, considering the geometry of the detail, its inspection, its method of fabrication and the direction of the stress relative to it. The basic design S-N curve (Figure 22), describing the fatigue for constant amplitude loadings, is given as equation 18:

$$\log N = \log K_2 - m \log \Delta \sigma \quad (18)$$

Where N is the predicted number of cycles to failure for the stress range $\Delta \sigma$, in N/mm^2 , while m is the negative inverse slope of S-N curve and $\log K_2$ indicates the interception of $\log N$ -axis by the curve. There is a knuckle located at 10^7 cycles.

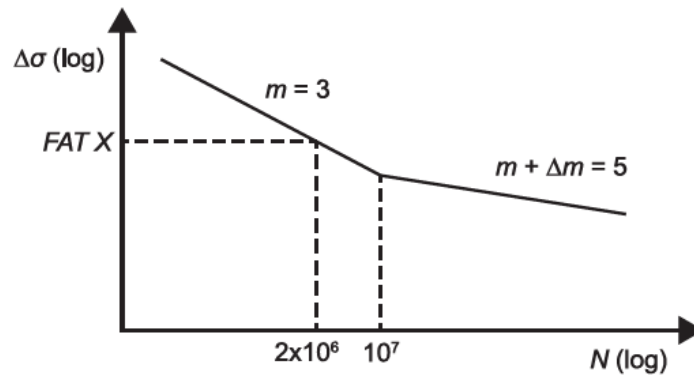


Figure 22 – FAT class S-N curves with FAT X number (DNVGL-CG-0129, 2019) Sec.2 [2.3]

The S-N curves for free plate edge or welded details (Figure 23) can be found in (DNVGL-CG-0129, 2019) Sec.2 [2.3]. These are applicable for normal and high strength steels used in construction of hull structures up to 500 N/mm^2 .

The reference stress ranges at $2 \cdot 10^6$ and 10^7 cycles are included (Table 1), also the structural stress concentration factor as derived from the hot spot method is included for reference. D-curve (FAT90) is the reference curve for the hot spot stress method and, in the case of WAPS, it shall be used for welded steel. For free plate edges, curve C FAT 125 shall be used, but curve B2 may also be accepted by the on a case-by-case basis.

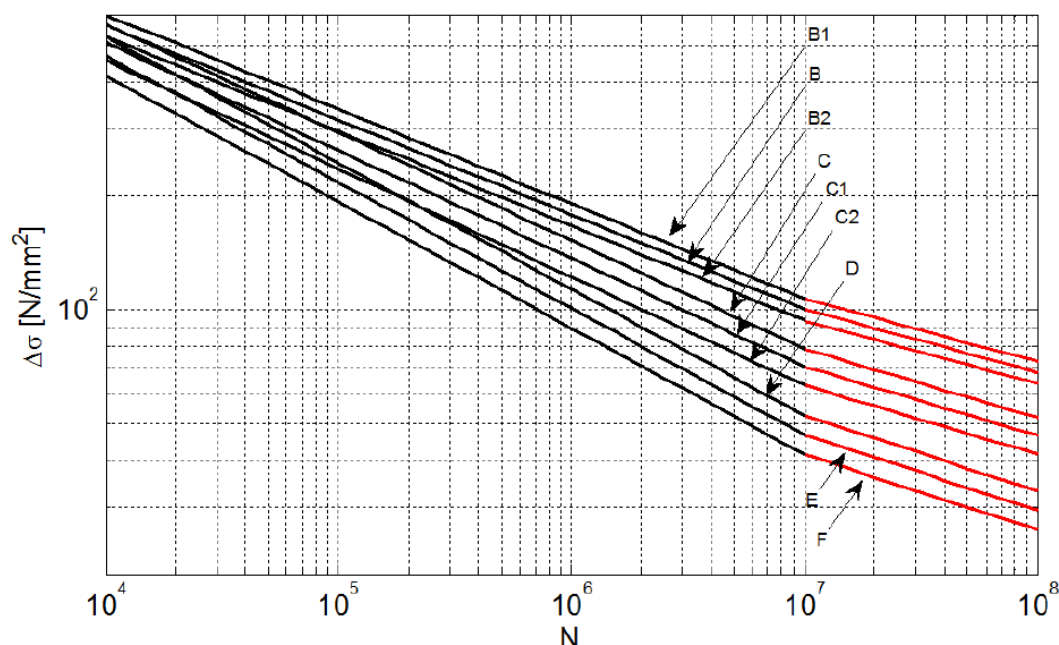


Figure 23 – S-N curves in air (DNVGL-CG-0129, 2019) Sec.2 [2.3]

Table 1 – S-N parameters for air (DNVGL-CG-0129, 2019) Sec.2 [2.3]

S-N Curve	Reference stress at $2 \cdot 10^6$ cycles (FAT)	Reference stress at 10^7 cycles (knuckle), $\Delta\sigma_q$	Structural stress concentration embedded in the detail and taken at $2 \cdot 10^6$ (10^7) cycles	$N \leq 10^7$		$N > 10^7$	
	N/mm ²	N/mm ²		$\log K_2$	m	$\log K_2$	$m + \Delta m$
B	150	100.31	0.60 (0.52)	15.005	4	19.008	6
B2	140	93.62	0.64 (0.56)	14.886	4	18.828	6
C	125	78.92	0.72 (0.67)	13.640	3.5	17.435	5.5
C1	112	70.72	0.80 (0.74)	13.473	3.5	17.172	5.5
C2	100	63.14	0.90 (0.83)	13.301	3.5	16.902	5.5
D	90	52.63	1.00 (1.00)	12.164	3	15.606	5
E	80	46.78	1.13 (1.13)	12.010	3	15.350	5
F	71	41.52	1.27 (1.27)	11.855	3	15.091	5
FAT	X	$0.585 \cdot X$	$90/X$ ($90/X$)	$6.301 + 3 \cdot \log(X)$	3	$7 + 5 \cdot \log(0.585 \cdot X)$	5

The S-N curves for welded joints include the effect of the local weld notch for the hot spot approach. For the nominal stress approach, i.e., FAT class S-N curves, also the detail itself is included (DNVGL-CG-0129, 2019) Sec.2 [2.3].

3.3.2. Fatigue Damage

Fatigue assessment may be carried out by Palmgren-Miner's rule, estimating the linear cumulative fatigue damage D from partial damages at different stress levels i (equation 19):

$$D = \sum_{i=1}^{n_{tot}} \frac{n_i}{N_i} \quad (19)$$

The number of load cycles, n_i , is determined by the stress spectrum. The spectrum is subdivided into i blocks for numerical analysis, each containing n_i stress cycles for stress ranges $\Delta\sigma_i$, totalizing n_{tot} stress range blocks. These are compared to S-N curves, composed by the number of endured stress cycles, N_i , for the same stress spectrum with the respective stress ranges (Figure 24).

Failure occurs when the limit damage sum is reached, being usually defined between 0.5 and 1.0 (Fricke W., 2017). The acceptance criteria to the damage are given by the rules.

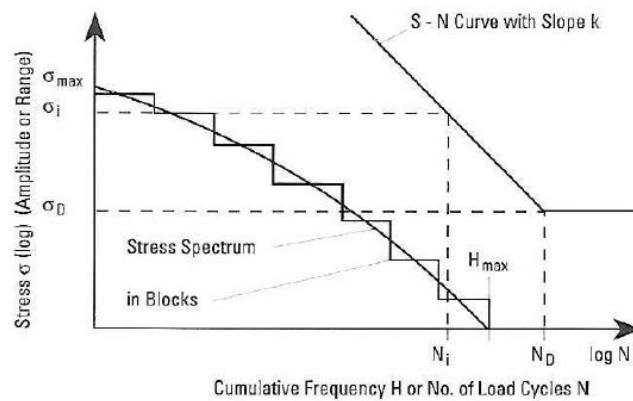


Figure 24 – Palmgren-Miner's rule for stress spectrum (Fricke, Petershagen, & Paetzold, 1997)

Moreover, when assessing the fatigue strength, the time in corrosive and in-air environment, the time in different loading conditions and the time in port need to be accounted

Regarding hull structures, the design fatigue life is divided into two time periods due to limitation of the corrosion protection. It is assumed that the corrosion protection is effective for a limited number of years during which the structural details are exposed to in-air environment. During the remaining part of the design life, the structural details are unprotected, as specified in (DNVGL-CG-0129, 2019) Sec.3 [3].

However, considering steel for the pedestal of the WAPS, corrosion is neglected provided the steel is coated with suitable coating quality. It is also assumed that the details are not located in a compartment with corrosive environment. Foundation details below the deck should be analysed as belonging to the hull, therefore, (DNV-RU-SHIP Pt.3 Ch.9, 2021) can be utilized. As it is the usual case for hulls, design fatigue life shall be 25 years. This implies a design fatigue factor, D_{FF} , or principal safety factor set to 1.0. In the sense of the cumulative fatigue damage, D , it means that this shall be less than or equal to 1.0 during the design fatigue life. In special cases, based on agreement with the society, a higher D_{FF} may be used. A D_{FF} of 2 implies 50 years design life rather than 25, or a cumulative damage of 0.5 rather than 1.0.

4. FATIGUE LOADS AND STRESS RANGES

Different from other structural limit states, fatigue does not deal with extreme loads. The fatigue damage depends on dynamic loads acting on the structure and, thus, its limit state is defined by a threshold of the damage accumulation. For this assessment, sporadic extreme loads are not relevant, being the analysis centred in more frequent loads, even if they present a small magnitude.

Resulting cyclic stresses in the structure arise from different excitement forces. These can be generated by weather or by the own ship machinery, for example. Therefore, it is important to determine which ones are relevant for evaluating the fatigue still in the design phase, avoiding problems due to damage accumulation during operation.

As ships spend a great amount of their lifetime navigating at the sea, it is not difficult to suspect that much of the fatigue damage comes from inertial loads induced by ship motions. The accelerations induced by the ship in waves affect the whole structure, especially the parts more distant from amidships and centreline. Such effects also affect the comfort of the crew and, so, the captain tries to avoid more extreme situations, but ships are, inevitably, affected by waves at some level.

However, cranes and other tall structures on deck are also susceptible to wind. This cannot be different for wind assisted propulsion systems since they, basically, generate thrust force from the wind itself. Different wind aspects and effects, as turbulence and vortex induced vibrations, might be considered according to the analysis level.

Moreover, vibrations may arise from the own WAPS operation (as in rotor sails), machinery system or propeller. This, nevertheless, is very difficult to be assessed during design phase and can be analysed separately. The levels of vibration shall be confirmed through measurements (DNV-RU-SHIP Pt.6 Ch.2, 2021) Sec.12 [3.1], and excessive vibration levels shall be mitigated.

The two main loads to be considered are, then, inertial and wind ones. These are described in more details within this section.

4.1. Inertial Loads

Inertial loads, as stated before, arise from ship motions. They can be calculated by different approaches, from more simplistic to more complex ones, according to the level of the design and information available:

- Envelope accelerations
- Equivalent design approach
- Direct hydrodynamics calculation

4.1.1. Envelope Accelerations

Envelope acceleration is the most simplistic approach and, for this reason, also the most conservative. It considers vertical, longitudinal and transverse accelerations and applies them in worst way for any combination with wind heading (Table 2), from (DNV-RU-SHIP Pt.3 Ch.4, 2021) Section 3 [3.3.4]. This considers always the worst-case regarding ship motions and, therefore, leads to a more conservative result (a higher damage).

Table 2 – Load combinations for envelope accelerations, from (DNV-RU-SHIP Pt.3 Ch.4, 2021) Section 3 [3.3.4]

Load combination	$a_{x-U}^{2)}$	$a_{y-U}^{2)}$	a_{z-U}
Head sea 1	a_{x-env}	0	$a_{z-env-pitch}$
Head sea 2 ¹⁾	a_{x-env}	0	$- a_{z-env-pitch}$
Beam sea 1	0	a_{y-env}	$a_{z-env-roll}$
Beam sea 2 ¹⁾	0	a_{y-env}	$- a_{z-env-roll}$
Oblique sea 1	$0.6 a_{x-env}$	$0.6 a_{y-env}$	a_{z-env}
Oblique sea 2 ¹⁾	$0.6 a_{x-env}$	$0.6 a_{y-env}$	$- a_{z-env}$
¹⁾ Load combination is only applicable for uplift conditions.			
²⁾ The horizontal accelerations shall be applied in the direction(s) giving maximum response.			

The extreme accelerations a_{x-env} , a_{y-env} and a_{z-env} are calculated at probability level of exceedance of 10^{-8} , resulting in a stress level $\Delta\sigma_0$. This value with Weibull slope parameter ξ^* sets the stress range spectrum.

To calculate the slope, first the downscaling factor f_p is calculated from (DNV-RU-SHIP Pt.3 Ch.4, 2021), Sec.3 [2.2.4], as showed in equation 20:

$$f_p = f_R [0.23 - 4f_T B \cdot 10^{-4}] \quad (20)$$

Where B is the vessel beam moulded, f_T depends on the loading condition and f_R is the operational (routing) factor.

The ship can operate at different loading conditions. Therefore, the inertia should be calculated for relevant cases, like ballast and full load, separately. For convenience, f_T draught ratio) may be taken as 0.5.

The inertial loads are specified for extreme values, which is not the case for fatigue loads. For these, an operational factor $f_R = 0.76$ shall be applied to the inertia-based stress, as seen in (DNV-RU-SHIP Pt.3 Ch.9, 2021), Section 4 [4.3].

Then, the Weibull slope parameter ξ^* is calculated from (DNVGL-CG-0129, 2019) Appendix C [1], as (equation 21):

$$\xi^* = \log_{10}(0.25) / \log_{10}(f_p) \quad (21)$$

By last, based on ξ^* , the number of cycles n and the 10^{-8} extreme response, the inertia induced stress histogram shall be established as in equation 22 from equation 17:

$$\Delta\sigma = \Delta\sigma_0 \left[1 - \frac{\log n}{\log n_0} \right]^{1/\xi^*} \quad (22)$$

Where n is the number of cycles exceeding $\Delta\sigma$ and n_0 is the total number of cycles associated with the stress range level $\Delta\sigma_0$.

The worst acceleration case can be combined with wind force in the same direction for a very conservative approach. In such situation, the worst loading condition can be used for a time span of 50% of the lifetime.

Such method can be useful when wind loads are dominating, and the mast structure is light. In this scenario, inertial loads are less important and may be less determinant for the fatigue design.

As a practical alternative to using the load spectrum, the inertia and wind loads can be derived by the downscaling factor f_p calculated at 10^{-2} probability level of exceedance and combined with a 0.6 factor. This is used as input into the fatigue damage calculations in (DNVGL-CG-0129, 2019) Sec.3 [3.3], provided that it is documented that the wind induced fatigue damage is also dominating at 10^{-2} probability level of exceedance, so that the Weibull shape parameter still can be set to 1.0.

More complex approaches, however, are necessary for cases where ship motions dominate. Refined approaches are not so simple, but they lead to less conservative results, which are the aim of the fatigue assessment. Different from other design limit states, fatigue does not need to be regarded as so conservative depending on the detail location and maintenance ease.

4.1.2. Equivalent Design Approach

In a more physical approach, the accelerations in the extreme case (10^{-8} probability level of exceedance) for the vertical, transverse and longitudinal motions are considered from the equivalent design waves, as seen in (DNV-RU-SHIP Pt.3 Ch.4, 2021), Sec.3 [3.2], for equations 23-25:

Longitudinal acceleration

$$a_X = f_\beta [(-C_{XG}g \sin \varphi) + C_{XS}a_{surge} + C_{XP}a_{pitch}(z - R)] \quad (23)$$

Transversal acceleration

$$a_Y = f_\beta [C_{YG}g \sin \theta + C_{YS}a_{sway} + C_{YR}a_{roll}(z - R)] \quad (24)$$

Vertical acceleration

$$a_Z = f_\beta [C_{ZH}a_{heave} + C_{ZR}a_{roll}y + C_{ZP}a_{pitch}(x - 0.45L)] \quad (25)$$

For this, there are several sectors for inertia, where “C” factors (Table 3, Table 4, Table 5). represent load combination factors to achieve scaled values (for each acceleration component), found in (DNV-RU-SHIP Pt.3 Ch.4, 2021) Sec.2 [2.2.1]. Phasing between the inertia components is represented by signs.

The headings for these equivalent design waves are represented by 8 sectors of 45 degrees:

- HSM – Head sea
- HSA – Bow quartering sea from port and starboard
- BSR – Beam sea from port and starboard side
- OST – Oblique following sea from port and starboard
- FSM – Following sea

The stress range is represented by the difference between cross and through for each equivalent design wave. Moreover, the inertia may be regarded as constant within a sector, or it may be interpolated between sectors to a finer resolution on headings. Once again, the downscaling factor f_p is calculated from (DNV-RU-SHIP Pt.3 Ch.4, 2021), Section 3 [2.2.4] and the Weibull slope parameter from (DNVGL-CG-0129, 2019) Appendix C.

Table 3 – Load combination factors for HSM, HSA and FSM load cases, (DNV-RU-SHIP Pt.3 Ch.4, 2021) Sec.2 [2.2.1]

Load component		LCF	HSM-1	HSM-2	HSA-1	HSA-2	FSM-1	FSM-2
Hull girder loads	M_{WV}	C_{WV}	-1	1	-0.7	0.7	$-0.4f_T - 0.6$	$0.4f_T + 0.6$
	Q_{WV}	C_{QW}	$-1.0f_{ip}$	$1.0f_{ip}$	$-0.6f_{ip}$	$0.6f_{ip}$	$-1.0f_{ip}$	$1.0f_{ip}$
	M_{WH}	C_{WH}	0	0	0	0	0	0
	M_{WT}	C_{WT}	0	0	0	0	0	0
Longitudinal accelerations	a_{surge}	C_{XS}	$0.6 - 0.2f_T$	$0.2f_T - 0.6$	0.2	-0.2	$0.2 - 0.4f_T$	$0.4f_T - 0.2$
	$a_{pitch-x}$	C_{XP}	$-0.15-L_1/300$	$0.15+L_1/300$	-1.0	1.0	0.15	-0.15
	$g \sin\phi$	C_{XG}	0.6	-0.6	$0.4f_T + 0.1$	$-0.4f_T - 0.1$	-0.2	0.2
Transverse accelerations	a_{sway}	C_{YS}	0	0	0	0	0	0
	a_{roll-y}	C_{YR}	0	0	0	0	0	0
	$g \sin\theta$	C_{YG}	0	0	0	0	0	0
Vertical accelerations	a_{heave}	C_{ZH}	$0.5f_T - 0.15$	$0.15 - 0.5f_T$	0.4	-0.4	0	0
	a_{roll-z}	C_{ZR}	0	0	0	0	0	0
	$a_{pitch-z}$	C_{ZP}	-0.7	0.7	-1.0	1.0	0.15	-0.15

Table 4 – Load combination factors for BSR and BSP load cases, (DNV-RU-SHIP Pt.3 Ch.4, 2021) Sec.2 [2.2.1]

Load component		LCF	BSR-1P	BSR-2P	BSR-1S	BSR-2S	BSP-1P	BSP-2P	BSP-1S	BSP-2S
Hull girder loads	M_{WV}	C_{WV}	$0.1 - 0.2f_T$	$0.2f_T - 0.1$	$0.1 - 0.2f_T$	$0.2f_T - 0.1$	$0.3 - 0.8f_T$	$0.8f_T - 0.3$	$0.3 - 0.8f_T$	$0.8f_T - 0.3$
	Q_{WV}	C_{QW}	$(0.1 - 0.2f_T) f_{ip}$	$(0.2f_T - 0.1) f_{ip}$	$(0.1 - 0.2f_T) f_{ip}$	$(0.2f_T - 0.1) f_{ip}$	$(0.3 - 0.8f_T) f_{ip}$	$(0.8f_T - 0.3) f_{ip}$	$(0.3 - 0.8f_T) f_{ip}$	$(0.8f_T - 0.3) f_{ip}$
	M_{WH}	C_{WH}	$1.2 - 1.1f_T$	$1.1f_T - 1.2$	$1.1f_T - 1.2$	$1.2 - 1.1f_T$	$0.7 - 0.7f_T$	$0.7f_T - 0.7$	$0.7f_T - 0.7$	$0.7 - 0.7f_T$
	M_{WT}	C_{WT}	0	0	0	0	0	0	0	0
Longitudinal accelerations	a_{surge}	C_{XS}	0	0	0	0	0	0	0	0
	$a_{pitch-x}$	C_{XP}	0	0	0	0	$0.1 - 0.3f_T$	$0.3f_T - 0.1$	$0.1 - 0.3f_T$	$0.3f_T - 0.1$
	$g \sin\phi$	C_{XG}	0	0	0	0	$0.3f_T - 0.1$	$0.1 - 0.3f_T$	$0.3f_T - 0.1$	$0.1 - 0.3f_T$
Transverse accelerations	a_{sway}	C_{YS}	$0.2 - 0.2f_T$	$0.2f_T - 0.2$	$0.2f_T - 0.2$	$0.2 - 0.2f_T$	-0.9	0.9	0.9	-0.9
	a_{roll-y}	C_{YR}	1	-1	-1	1	0.3	-0.3	-0.3	0.3
	$g \sin\theta$	C_{YG}	-1	1	1	-1	-0.2	0.2	0.2	-0.2
Vertical accelerations	a_{heave}	C_{ZH}	$0.7 - 0.4f_T$	$0.4f_T - 0.7$	$0.7 - 0.4f_T$	$0.4f_T - 0.7$	1	-1	1	-1
	a_{roll-z}	C_{ZR}	1	-1	-1	1	0.3	-0.3	-0.3	0.3
	$a_{pitch-z}$	C_{ZP}	0	0	0	0	$0.1 - 0.3f_T$	$0.3f_T - 0.1$	$0.1 - 0.3f_T$	$0.3f_T - 0.1$

Table 5 – Load combination factors for OST and OSA load cases, (DNV-RU-SHIP Pt.3 Ch.4, 2021)

Sec.2 [2.2.1]

Load component		LCF	OST-1P	OST-2P	OST-1S	OST-2S	OSA-1P	OSA-2P	OSA-1S	OSA-2S
Hull girder loads	M_{WV}	C_{WV}	$-0.3 - 0.2f_T$	$0.3 + 0.2f_T$	$-0.3 - 0.2f_T$	$0.3 + 0.2f_T$	$0.75 - 0.5f_T$	$-0.75 + 0.5f_T$	$0.75 - 0.5f_T$	$-0.75 + 0.5f_T$
	Q_{WV}	C_{QW}	$(-0.35 - 0.2f_T) f_{ip}$	$(0.35 + 0.2f_T) f_{ip}$	$(-0.35 - 0.2f_T) f_{ip}$	$(0.35 + 0.2f_T) f_{ip}$	$(0.6 - 0.4f_T) f_{ip}$	$(-0.6 + 0.4f_T) f_{ip}$	$(0.6 - 0.4f_T) f_{ip}$	$(-0.6 + 0.4f_T) f_{ip}$
	M_{WH}	C_{WH}	-1.0	1.0	1.0	-1.0	$0.55 + 0.2f_T$	$-0.55 - 0.2f_T$	$-0.55 - 0.2f_T$	$0.55 + 0.2f_T$
	M_{WT}	C_{WT}	$-f_{ip-OST}$	f_{ip-OST}	f_{ip-OST}	$-f_{ip-OST}$	$-f_{ip-OSA}$	f_{ip-OSA}	f_{ip-OSA}	$-f_{ip-OSA}$
Longitudinal accelerations	a_{surge}	C_{XS}	$0.1f_T - 0.15$	$0.15 - 0.1f_T$	$0.1f_T - 0.15$	$0.15 - 0.1f_T$	-0.45	0.45	-0.45	0.45
	$a_{pitch-x}$	C_{XP}	$0.7 - 0.3f_T$	$0.3f_T - 0.7$	$0.7 - 0.3f_T$	$0.3f_T - 0.7$	0.5	-0.5	0.5	-0.5
	$g_{sin\phi}$	C_{XG}	$0.2f_T - 0.45$	$0.45 - 0.2f_T$	$0.2f_T - 0.45$	$0.45 - 0.2f_T$	-0.8	0.8	-0.8	0.8
Transverse accelerations	a_{sway}	C_{YS}	0	0	0	0	$-0.2 - 0.1f_T$	$0.2 + 0.1f_T$	$0.2 + 0.1f_T$	$-0.2 - 0.1f_T$
	a_{roll-y}	C_{YR}	$0.4f_T - 0.25$	$0.25 - 0.4f_T$	$0.25 - 0.4f_T$	$0.4f_T - 0.25$	$0.3 - 0.2f_T$	$0.2f_T - 0.3$	$0.2f_T - 0.3$	$0.3 - 0.2f_T$
	$g_{sin\theta}$	C_{YG}	$0.1 - 0.2f_T$	$0.2f_T - 0.1$	$0.2f_T - 0.1$	$0.1 - 0.2f_T$	$0.1f_T - 0.2$	$0.2 - 0.1f_T$	$0.2 - 0.1f_T$	$0.1f_T - 0.2$
Vertical accelerations	a_{heave}	C_{ZH}	$0.2f_T - 0.05$	$0.05 - 0.2f_T$	$0.2f_T - 0.05$	$0.05 - 0.2f_T$	$-0.2f_T$	$0.2f_T$	$-0.2f_T$	$0.2f_T$
	a_{roll-z}	C_{ZR}	$0.4f_T - 0.25$	$0.25 - 0.4f_T$	$0.25 - 0.4f_T$	$0.4f_T - 0.25$	$0.3 - 0.2f_T$	$0.2f_T - 0.3$	$0.2f_T - 0.3$	$0.3 - 0.2f_T$
	$a_{pitch-z}$	C_{ZP}	$0.7 - 0.3f_T$	$0.3f_T - 0.7$	$0.7 - 0.3f_T$	$0.3f_T - 0.7$	1.0	-1.0	1.0	-1.0

4.1.3. Direct Hydrodynamics Calculation

By last, there are the direct hydrodynamic calculations, as in (DNVGL-CG-0130, 2018), which can use ship specific calculations with improved phase relations and amplitudes, besides choosing frequent loading conditions when inertia dominates the fatigue damage. By them, the accelerations at any point in the ship can be calculated and time series of the inertia induced stress can be established. Another advantage is carrying out the calculations for a specific trade route, based on improved environmental description, selected loading conditions and combination of wind and wave induced stress.

4.2. Wind loads**4.2.1. Global Wind Matrix**

Wind propulsion systems are innovative mechanical energy efficient technologies for reducing the CO2 emissions of ships, therefore, enhancing their Energy Efficiency Design Index (EEDI). Thus, a global wind probability methodology needs to be adopted to calculate the wind propulsion power of these systems and determine the ship specific EEDI (Marine

Environment Protection Committee, 2011). The results from this methodology can also be applied to estimate the fatigue damage for WAPS.

It presents some definitions:

- Wind speed is the speed of the wind in m/s measured at 10 m above sea level.
- Wind angle is the angle of the wind relative to the ship's heading at 10 m above sea level subdivided into 72 sectors of 5°-steps (0°, 5°, ..., 355°).
- The main global shipping network is a network of global shipping routes with the highest frequency of journeys.

For a wind propulsion system, it is irrelevant if the wind is coming from North or South. Only the wind angle relative to a ship's heading is of importance. Consequently, the wind directions given in the weather data are recalculated for ship headings on a trading route when applied to wind propulsion systems, where 0° means the ship's bow, 90° its starboard side, 180° the stern and 270° port side.

Regarding the global wind matrix, each element of it represents the probability of occurrence for the specific wind speed and wind angle relative to the ship. The sum of all matrix elements is one, representing 100% of all wind conditions.

About the results (ANNEX), they show that winds to the bow or the stern occur more often than winds to the sides. There are two possible reasons to explain this phenomenon: shipping routes and global weather systems are more East-West than North-South oriented; and shipping routes and winds are influenced by shorelines, so they tend to be parallel in some regions (Marine Environment Protection Committee, 2011).

4.2.2. Wind Profile

It is also important to always consider the height which the wind is measured and applied. The mean wind speed presents a variation according to the height above the ground or above the still water level. This wind speed profile can be represented by an idealised model profile. The most applied wind profile models are the logarithmic profile model, the power law model and the Frøya model (DNV-RP-C205, 2019) [2.3.2].

An acceptable wind profile is the power law one (equation 26) (DNV-RP-C205, 2019) [2.3.2.8]:

$$U(z) = U(H) \left(\frac{z}{H} \right)^\alpha \quad (26)$$

Where $\alpha = 0.12$ for wind on open sea with waves.

Another alternative is the Frøya wind speed profile, the more documented one for offshore locations and maritime conditions, being recommended for such locations. The Frøya wind speed profile is a special case of the logarithmic wind speed profile and includes a gust factor which allows for conversion of mean wind speeds between different averaging periods. This model, therefore, implies an expression for the most likely largest wind speed (gust) that can be used for converting a mean wind speed not only for different heights, but also for different averaging periods.

The following expression can be used for conversion of the one-hour mean wind speed U_0 at height H above the sea level to the mean wind speed U with averaging period T at height z above sea level (equation 27) (DNV-RP-C205, 2019) [2.3.2.11]:

$$U(T, z) = U_0 \cdot \left\{ 1 + C \cdot \ln \frac{z}{H} \right\} \cdot \left\{ 1 - 0.41 \cdot I_v(z) \ln \frac{T}{T_0} \right\} \quad (27)$$

Where $H = 10$ m, $T_0 = 1$ hour, $T < T_0$ and equations 28 and 29 apply:

$$C = 5.73 \cdot 10^{-2} \sqrt{1 + 0.148 U_0} \quad (28)$$

$$I_v = 0.06 * (1 + 0.043 U_0) * \left(\frac{z}{H} \right)^{-0.22} \quad (29)$$

This conversion, although useful for calculating the wind speed according to height and gustiness, delivers a single value. That is, it can show how the wind speed is changing along the height or the most likely gust, but not exactly how wind oscillates along the time. Regarding time, the conversion works between wind speed averaging periods is called gust factor, with increasing values for shorter averaging periods.

From this, it is possible to think that, knowing how WAPS and wind interact, it would be possible to find an averaging period which would give the highest response for the system. Then, it would be possible to calculate a gust and the loads generated by it. However, as it will be better described next, the gust from Frøya wind speed profile is a peak value.

4.2.3. *Gust Factor*

The mean wind speed is not very useful for fatigue as the latter occurs due to cyclic stresses. For this reason, wind variations should be considered. However, this is not straightforward and different terms apply for such variations, as turbulence and gust factor.

Turbulence are shorter period fluctuations in natural wind (World Meteorological Organisation, 2008). It would be the expected variation for a shorter random sample of the wind speed around the true mean one. Normally mean wind is estimated from a 10-minute average (World Meteorological Organisation, 2008) and, so, turbulence is the natural variability of the wind speed about the mean wind speed in this period, characterised by a standard deviation (DNV-RP-C205, 2019).

“Gust” is defined as the highest average wind speed of shorter averaging period within some longer period of observation. The mean wind speed is the one for the observation period while the gust speed is the highest average for a shorter period (gust period). The “gust factor” is then a theoretical conversion between an estimate of the mean wind speed for a stated observation period and the expected highest gust wind speed of a given duration within that period (World Meteorological Organisation, 2008).

The gust factor, $G(z)$, can be calculated for different distances from the sea surface based on the ratio (equation 30):

$$G(z) = U(T, z)/U(z) \quad (30)$$

So, while turbulence is an expected natural variation of the wind speed for shorter averaging periods within an observation period (a range of expected values), gust is highest value to be expected for a shorter sample. Gusts would, thus, give peak values for the loads within a period, useful for ultimate loads, but not for fatigue. Fatigue would depend on the effects of the shorter periods, so, on the turbulence.

This wind indicates that fatigue for WAPS requires a dynamic analysis, considering the time variation of wind forces, as it happens for other wind exposed equipment and objects sensitive to varying wind loads (DNV-RP-C205, 2019) [5.6]. The variation of the wind field can be described as the sum of a sustained wind component and a fluctuating gust component, which can be described by a wind spectrum. For wind over water, Frøya model spectral density is recommended (DNV-RP-C205, 2019) [2.3.4].

From this it is possible to generate multiple wind time-series, apply them for a given WAPS and assess their damage by counting the hysteresis cycles via rainflow, similarly to what is done to wind turbines. However, such procedure is not practical for estimating fatigue still at an early project phase. Another aspect is how to combine the loads arising from the wind with the loads induced by waves.

Considering these aspects and the necessity to have a simple method to assess the fatigue loads, a fatigue gust factor is suggested. Such factor can be applied to the mean wind speed to calculate the load variation related to the wind fluctuation. The general procedure to achieve this factor is explained in the following and can be replicated for different WAPS.

In summary, a wind velocity history is generated utilizing the Frøya energy spectrum for a range of mean wind speeds and heights. Then, it is straightforward to generate a stress history and count the stress cycles with rainflow method. The damage caused by these stress cycles can be assessed and, considering a defined number of cycles, it is possible to go backwards on this procedure, finding an equivalent stress and, finally, an equivalent gust factor.

Such procedure can be applied for a generalized wind propulsion system. Moreover, considering the combination of wind and wave loads, the number of cycles for calculating the factor is obtained from the roll period. With different wind speeds, equipment height and roll period, it is possible to analyse how the factor relates to each one of these parameters and develop a formula to easily find an adequate fatigue factor for any WAPS.

The fatigue gust factor procedure can be, therefore, implemented in Matlab or a similar software to generate random time series and calculate a fatigue gust factor. The algorithm is explained next:

1. Generate wind speed history (for different mean wind speed, U_0 , and height, z)
 - a. Frøya model spectral density (DNV-RP-C205, 2019) [2.3.4.12] to generate wind speed (equations 31-35):

$$f = 0.001:0.001:1 \quad (31)$$

$$\tilde{f}_i = 172 * f_i * \left(\frac{z}{10}\right)^{\frac{2}{3}} * \left(\frac{U_0}{10}\right)^{-0.75} \quad (32)$$

$$S_U(f_i) = 320 * \frac{\left(\frac{U_0}{10}\right)^2 \left(\frac{z}{10}\right)^{0.45}}{\left(1 + \tilde{f}_i^n\right)^{\frac{5}{3n}}} \quad (33)$$

$$df_i = \frac{f_i - f_{i-1}}{2} + \frac{f_{i+1} - f_i}{2} \quad (34)$$

$$A_i = S_U(f_i) * df_i \quad (35)$$

- $n = 0.468$.
- U_0 is the 1-hour mean wind speed at 10 m height in units of m/s.
- z is the height above sea level in units of m (to be assumed at midspan).
- The expressions should not be extrapolated for heights above approximately 100 m. Possible influences from geostrophic winds down to about 100 m height emphasises the importance of observing this restriction (DNV-RP-C205, 2019) [2.3.2.14].

b. Generate wind speed time series for 1-hour (3600s) (equations 36-40):

$$t = 0:1:3600 \quad (36)$$

$$\varphi_i = rand() * 2\pi \quad (37)$$

$$v_i(t) = A_i * \cos(2\pi * f_i * t + \varphi_i) \quad (38)$$

$$V(t) = \sum_i v_i(t) \quad (39)$$

$$U(t) = U_0 + V(t) * \frac{std(v)}{I_H * U_0} \quad (40)$$

From (DNV-RP-C205, 2019) [2.3.2.11] (equation 41):

$$I_H = 0.06 * (1 + 0.043U_0) * \left(\frac{z}{H}\right)^{-0.22} \quad (41)$$

2. Generate stress history from wind speed (equation 42-45):

$$Wind\ Load = \frac{1}{2} * \rho * C * S * U^2 \quad (42)$$

$$Moment = Wind\ Load * arm \text{ (where } arm = z) \quad (43)$$

$$Stress = \frac{Moment * y}{I} \quad (44)$$

$$\sigma = \frac{1}{2} * \frac{\rho * C * S * U^2 * z * y_{max}}{I} * \frac{1}{10^6} [N/mm^2] \quad (45)$$

- ρ, C, S, y_{max}, I not considered since they are constant for a given WAPS
- $\frac{1}{2}$ also not considered, since it is constant
- $* 10^{-6}$ kept due to unit conversion to $[N/mm^2]$ (equation 46):

$$\frac{\left[\frac{kg}{m^3}\right] * [-] * [m^2] * \left[\frac{m}{s}\right]^2 * [m] * [m]}{[m^4]} = \left[\frac{kg * m^6}{m^7 * s^2}\right] = \left[\frac{N}{m^2}\right] = \left[\frac{N}{10^6 * mm^2}\right] \quad (46)$$

3. Count stress cycles with rainflow (Figure 25 and Figure 26):

- Rainflow* counting (MathWorks, n.d.) to get stress range bins and cycles at each bin
- Sum cycles at same stress range interval (different cycle average stress)
- For damage calculation, utilize mean stress range of each bin
- Each stress range $\Delta\sigma_i$ presents corresponding n_i cycles

*Matlab utilizes a slightly modified rainflow method, given by ASTM E 1049-85, that recommends the three-point method (Lee & Tjhung, 2012).

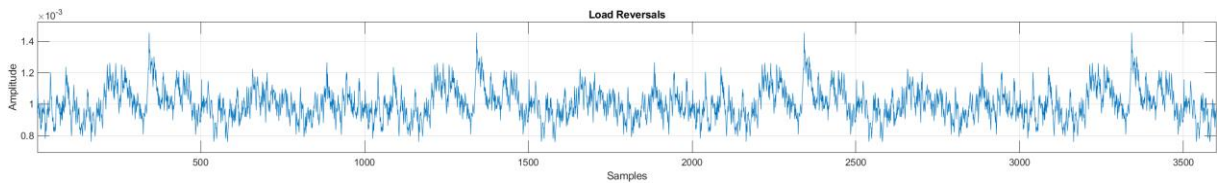


Figure 25 – Load history and reversals

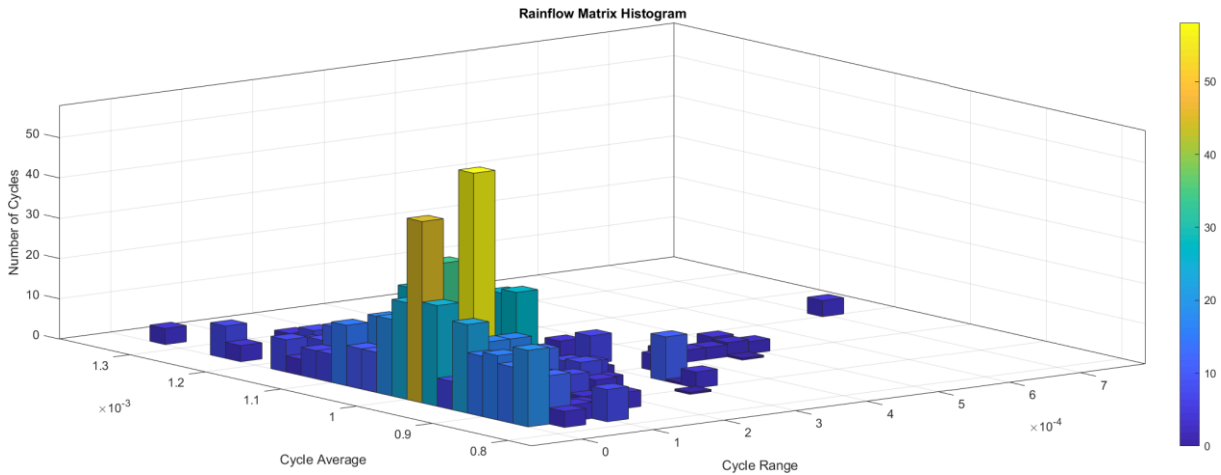


Figure 26 – Rainflow matrix histogram (cycle average x cycle range)

4. Assess fatigue damage:

- As in (DNVGL-CG-0129, 2019) Sec.2 [2.3], Curve D (air), for $N \leq 10^7$ (equations 47 and 48):

$$m = 3 \quad (47)$$

$$\log K_2 = 12.164 \quad (48)$$

Considering a single slope, thus, conservative approach.

b. Calculate damage (equations 49-51):

$$\log N_i = \log K_2 - m \log \Delta \sigma_i \quad (49)$$

$$N_i = 10^{\log K_2 - m \log(\Delta \sigma_i)} \quad (50)$$

$$D = \sum_i \frac{n_i}{N_i} \quad (51)$$

Where n_i is the number of cycles for each stress range bin $\Delta \sigma_i$.

5. Get equivalent stress (equations 52-54):

$$n_{eq} = \frac{1 \text{ hour}}{T_\theta} \quad (52)$$

Where T_θ is the roll period:

$$D = \frac{n_{eq}}{N_{eq}} \quad (53)$$

$$\Delta \sigma_{eq} = 10^{\frac{\log K_2 - \log N_{eq}}{m}} \quad (54)$$

Roll period is taken from (DNV-RU-SHIP Pt.3 Ch.4, 2021) Sec.3 [2.1.1] (equation 55):

$$T_\theta = \frac{2.3\pi k_r}{\sqrt{g GM}} \quad (55)$$

6. Get gust factor (equations 56-64):

a. Considering $U_{max} = (1 + gust)U_0$ and $U_{min} = (1 - gust)U_0$

$$\sigma = \frac{1}{2} * \frac{\rho * C * S * U^2 * z * y_{max}}{I} * \frac{1}{10^6} [N/mm^2] \quad (56)$$

$$\Delta \sigma = \sigma_{max} - \sigma_{min} \quad (57)$$

$$\Delta \sigma = \sigma(U_{max}) - \sigma(U_{min}) \quad (58)$$

$$\Delta \sigma = ((1 + gust)^2 - (1 - gust)^2) * \frac{1}{2} * \frac{\rho * C * S * U_0^2 * z * y_{max}}{I} * \frac{1}{10^6} \quad (59)$$

$$\Delta \sigma = ((1 + gust)^2 - (1 - gust)^2) * \sigma(U_0) \quad (60)$$

$$\Delta \sigma = 4 * gust * \sigma(U_0) \quad (61)$$

$$gust = \frac{\Delta \sigma}{4 * \sigma(U_0)} \quad (62)$$

Table 7 – Fatigue Gust Factor calculated for 10m height (100 repetitions), T4 stands for roll period

Fatigue Gust Factor		T4 [s]																						
		5	6	7	8	9	10	11	12	13	14	15	16	17	18	19	20	21	22	23	24	25		
U0 [m/s]	1	0,01	0,01	0,01	0,01	0,01	0,01	0,01	0,01	0,01	0,01	0,01	0,01	0,01	0,01	0,01	0,01	0,01	0,01	0,01	0,01	0,01		
	2	0,01	0,02	0,02	0,02	0,02	0,02	0,02	0,02	0,02	0,02	0,02	0,02	0,02	0,02	0,02	0,02	0,02	0,02	0,02	0,02	0,02		
	3	0,02	0,02	0,02	0,02	0,02	0,03	0,03	0,03	0,03	0,03	0,03	0,03	0,03	0,03	0,03	0,03	0,03	0,03	0,03	0,03	0,03		
	4	0,03	0,03	0,03	0,03	0,03	0,03	0,03	0,03	0,04	0,04	0,04	0,04	0,04	0,04	0,04	0,04	0,04	0,04	0,04	0,04	0,04		
	5	0,03	0,03	0,03	0,04	0,04	0,04	0,04	0,04	0,04	0,04	0,04	0,04	0,05	0,05	0,05	0,05	0,05	0,05	0,05	0,05	0,05		
	6	0,03	0,04	0,04	0,04	0,04	0,04	0,04	0,05	0,05	0,05	0,05	0,05	0,05	0,05	0,05	0,05	0,06	0,06	0,06	0,06	0,06		
	7	0,04	0,04	0,04	0,04	0,05	0,05	0,05	0,05	0,05	0,05	0,05	0,06	0,06	0,06	0,06	0,06	0,06	0,06	0,06	0,06	0,07		
	8	0,04	0,04	0,05	0,05	0,05	0,05	0,05	0,06	0,06	0,06	0,06	0,06	0,06	0,06	0,06	0,06	0,07	0,07	0,07	0,07	0,07		
	9	0,04	0,05	0,05	0,05	0,05	0,06	0,06	0,06	0,06	0,06	0,06	0,07	0,07	0,07	0,07	0,07	0,07	0,07	0,07	0,08	0,08		
	10	0,05	0,05	0,05	0,06	0,06	0,06	0,06	0,06	0,07	0,07	0,07	0,07	0,07	0,07	0,07	0,08	0,08	0,08	0,08	0,08	0,08		
	11	0,05	0,05	0,06	0,06	0,06	0,06	0,07	0,07	0,07	0,07	0,07	0,07	0,08	0,08	0,08	0,08	0,08	0,08	0,08	0,08	0,09		
	12	0,05	0,06	0,06	0,06	0,06	0,07	0,07	0,07	0,07	0,07	0,08	0,08	0,08	0,08	0,08	0,08	0,08	0,09	0,09	0,09	0,09		
	13	0,05	0,06	0,06	0,06	0,07	0,07	0,07	0,07	0,08	0,08	0,08	0,08	0,08	0,08	0,09	0,09	0,09	0,09	0,09	0,09	0,09		
	14	0,06	0,06	0,06	0,07	0,07	0,07	0,07	0,08	0,08	0,08	0,08	0,08	0,09	0,09	0,09	0,09	0,09	0,09	0,09	0,10	0,10		
	15	0,06	0,06	0,07	0,07	0,07	0,07	0,08	0,08	0,08	0,08	0,08	0,09	0,09	0,09	0,09	0,09	0,09	0,10	0,10	0,10	0,10		
	20	0,07	0,07	0,07	0,08	0,08	0,08	0,09	0,09	0,09	0,09	0,10	0,10	0,10	0,10	0,10	0,10	0,11	0,11	0,11	0,11	0,11		
	25	0,07	0,08	0,08	0,08	0,09	0,09	0,09	0,10	0,10	0,10	0,10	0,10	0,11	0,11	0,11	0,11	0,11	0,12	0,12	0,12	0,12		
	30	0,07	0,08	0,08	0,09	0,09	0,09	0,10	0,10	0,10	0,11	0,11	0,11	0,11	0,11	0,12	0,12	0,12	0,12	0,12	0,13	0,13		
	35	0,08	0,08	0,09	0,09	0,09	0,10	0,10	0,10	0,11	0,11	0,11	0,11	0,12	0,12	0,12	0,12	0,13	0,13	0,13	0,13	0,13		
	40	0,08	0,08	0,09	0,09	0,10	0,10	0,10	0,11	0,11	0,11	0,11	0,12	0,12	0,12	0,12	0,13	0,13	0,13	0,13	0,13	0,14		
	45	0,08	0,09	0,09	0,09	0,10	0,10	0,11	0,11	0,11	0,11	0,12	0,12	0,12	0,12	0,13	0,13	0,13	0,13	0,13	0,14	0,14		
	50	0,08	0,09	0,09	0,10	0,10	0,10	0,11	0,11	0,11	0,12	0,12	0,12	0,12	0,13	0,13	0,13	0,13	0,13	0,14	0,14	0,14		

It is, thus, possible to create a formula for the fatigue gust factor in function of mean wind and roll period, assuming height as 10m. This formula is developed for a mean value since one does not seek to be too conservative regarding fatigue. The same reason explains why standard deviation is not considered, as it is of more relevance for extreme cases where a single event would be fatal for the structure, which is not the case of fatigue.

A formula (equation 65) is proposed for calculating the fatigue gust factor, G_R . The formula is fitted for wind speeds up to 15 m/s, slightly overestimating the values for slower wind speeds:

$$G_R(U_0, T_\theta) = (2,44 * \ln(U_0) + 0,14T_\theta) * 10^{-2} \quad (65)$$

G_R can be taken as constant over the height z .

For higher wind speeds (up to 50 m/s), there is the addition of a safety factor of 0.01.

The results from the application of the formula are summarized in Table 8:

Table 8 – Fatigue Gust Factor obtained by formula, T4 stands for roll period

Fatigue Gust Factor		T4 [s]																								
		5	6	7	8	9	10	11	12	13	14	15	16	17	18	19	20	21	22	23	24	25				
U0 [m/s]	1	0,01	0,01	0,01	0,01	0,01	0,01	0,02	0,02	0,02	0,02	0,02	0,02	0,03	0,03	0,03	0,03	0,03	0,03	0,03	0,03	0,04				
	2	0,02	0,03	0,03	0,03	0,03	0,03	0,03	0,03	0,04	0,04	0,04	0,04	0,04	0,04	0,04	0,05	0,05	0,05	0,05	0,05	0,05				
	3	0,03	0,04	0,04	0,04	0,04	0,04	0,04	0,04	0,05	0,05	0,05	0,05	0,05	0,05	0,05	0,06	0,06	0,06	0,06	0,06	0,06				
	4	0,04	0,04	0,04	0,05	0,05	0,05	0,05	0,05	0,05	0,05	0,05	0,06	0,06	0,06	0,06	0,06	0,06	0,06	0,07	0,07	0,07				
	5	0,05	0,05	0,05	0,05	0,05	0,05	0,05	0,06	0,06	0,06	0,06	0,06	0,06	0,06	0,07	0,07	0,07	0,07	0,07	0,07	0,07				
	6	0,05	0,05	0,05	0,05	0,06	0,06	0,06	0,06	0,06	0,06	0,06	0,06	0,07	0,07	0,07	0,07	0,07	0,07	0,08	0,08	0,08				
	7	0,05	0,06	0,06	0,06	0,06	0,06	0,06	0,06	0,07	0,07	0,07	0,07	0,07	0,07	0,07	0,07	0,08	0,08	0,08	0,08	0,08				
	8	0,06	0,06	0,06	0,06	0,06	0,06	0,07	0,07	0,07	0,07	0,07	0,07	0,07	0,07	0,08	0,08	0,08	0,08	0,08	0,08	0,09				
	9	0,06	0,06	0,06	0,06	0,07	0,07	0,07	0,07	0,07	0,07	0,07	0,08	0,08	0,08	0,08	0,08	0,08	0,08	0,09	0,09	0,09				
	10	0,06	0,06	0,07	0,07	0,07	0,07	0,07	0,07	0,07	0,08	0,08	0,08	0,08	0,08	0,08	0,08	0,09	0,09	0,09	0,09	0,09				
	11	0,07	0,07	0,07	0,07	0,07	0,07	0,07	0,08	0,08	0,08	0,08	0,08	0,08	0,08	0,09	0,09	0,09	0,09	0,09	0,09	0,09				
	12	0,07	0,07	0,07	0,07	0,07	0,07	0,08	0,08	0,08	0,08	0,08	0,08	0,08	0,09	0,09	0,09	0,09	0,09	0,09	0,09	0,10				
	13	0,07	0,07	0,07	0,07	0,08	0,08	0,08	0,08	0,08	0,08	0,08	0,08	0,09	0,09	0,09	0,09	0,09	0,09	0,09	0,10	0,10				
	14	0,07	0,07	0,07	0,08	0,08	0,08	0,08	0,08	0,08	0,08	0,09	0,09	0,09	0,09	0,09	0,09	0,09	0,10	0,10	0,10	0,10				
	15	0,07	0,07	0,08	0,08	0,08	0,08	0,08	0,08	0,08	0,09	0,09	0,09	0,09	0,09	0,09	0,09	0,10	0,10	0,10	0,10	0,10				
	20	0,09	0,09	0,09	0,09	0,10	0,10	0,10	0,10	0,10	0,10	0,10	0,11	0,11	0,11	0,11	0,11	0,11	0,11	0,12	0,12	0,12				
	25	0,10	0,10	0,10	0,10	0,10	0,10	0,10	0,11	0,11	0,11	0,11	0,11	0,11	0,12	0,12	0,12	0,12	0,12	0,12	0,12	0,12				
	30	0,10	0,10	0,10	0,10	0,11	0,11	0,11	0,11	0,11	0,11	0,11	0,12	0,12	0,12	0,12	0,12	0,12	0,12	0,13	0,13	0,13				
	35	0,10	0,11	0,11	0,11	0,11	0,11	0,11	0,11	0,11	0,12	0,12	0,12	0,12	0,12	0,12	0,12	0,13	0,13	0,13	0,13	0,13				
	40	0,11	0,11	0,11	0,11	0,11	0,11	0,12	0,12	0,12	0,12	0,12	0,12	0,12	0,13	0,13	0,13	0,13	0,13	0,13	0,13	0,14				
	45	0,11	0,11	0,11	0,11	0,12	0,12	0,12	0,12	0,12	0,12	0,12	0,13	0,13	0,13	0,13	0,13	0,13	0,13	0,14	0,14	0,14				
	50	0,11	0,11	0,12	0,12	0,12	0,12	0,12	0,12	0,12	0,13	0,13	0,13	0,13	0,13	0,13	0,13	0,13	0,14	0,14	0,14	0,14				

4.2.4. Vessel Speed

According to (DNVGL-CG-0130, 2018), for wave induced and inertial loads, the vessel speed used for fatigue damage predictions is taken as 2/3 of the maximum service speed. For wind, the vessel speed shall be assumed as 2/3 of the maximum service speed from head to ± 67.5 degrees off head sea, as especially head to bow quartering waves imply involuntary speed reduction. For other wind headings, the vessel speed shall be assumed as the maximum service speed.

4.2.5. Apparent Wind Heading and Speed

The wind angle provided by the global wind probability matrix is the angle of the wind relative to the ship's heading at 10 m above sea level, the true relative wind heading. However, in operation, there is a combination between the forward speed of the vessel and the true wind one. Hence, the apparent wind speed and the apparent wind heading shall be calculated as basis for load calculations.

It is also important to consider the wind profile. As the wind speed increases with distance from the sea surface, this also affects the apparent wind angle for different heights. It is

suggested, for simplification, to adopt the midspan of the sails as a reference height to calculate such effects.

4.2.6. Wind Load Application

As sails are tall structures and can present different shapes, it is also important to study the load's application point. For the foundation of the WAPS, the moment around the base is calculated and the equivalent height where wind speed may be predicted is regarded as representative for the whole sail height. However, wind speed profile is not the only relevant aspect as other parameters may vary depending on the sail design, as lift and drag coefficients, cord length, surface area and sail angle of attack. Therefore, their values shall be provided by the manufacturer for a more detailed analysis.

A detailed structural analysis requires calculating the wind loads and stresses along the sail height, what also gives the resultant forces along the mast. For the scope of the fatigue at the foundation, the wind loads on the sails shall be summarized for the entire sail area. The integration of all the wind loads on the sail accounts for the total load applied, while their weighted average provides the load's application point.

For simplification, the wind speed may be calculated at the midspan (vertically) of the sail as basis for both lift and drag forces. Considering the wind speed profiles, such value would be slightly conservative. However, to calculate the wind loads, speed is considered quadratically and there is also the moment generated by the wind force, which is affected by the height.

To calculate the moment generated by wind, the total wind force is applied at a single point, the centre of effort. This spot can be located at different heights according to the sail type. While for rigid sails it can be assumed at midspan (vertically), for soft sails of traditional design it may be as low as 0.38 of the sail height.

Therefore, it is important to verify if the simplification holds for estimating the moment at the base of the WAPS. Nevertheless, it is not easy to assume a precise point for the centre of effort and the wind speed assessment since the wind is varying with the height and the heights considered depend on the sail vertical span. Not only the height, but also the shape of the sail (rectangular or triangular) can affect a lot the final value.

This can be performed for a small set of sails, with variable sail spans and foundation heights, to verify the assumption. The values for the moment around the foundation for rectangular and triangular sails are calculated with the simplifications and compared to the results

obtained by integration. According to the sail shape, different heights are assumed for the centre of effort and for assessing the wind speed.

The parameters and results follow, with the results shown as a reason of the values obtained by simplifications over the ones obtained by integration:

- Sail height (vertical span): 30m, 40m, 50m
- Sail breadth: 10m
- Foundation height: 5m, 10m, 15m
- Rectangular sail (Table 9)
 - Wind speed and centre of effort at midspan

Table 9 – Moment comparison for rectangular sails

Foundation height (m)	Sail height (m)		
	30	40	50
5	97%	97%	97%
10	98%	97%	97%
15	98%	98%	97%

- Triangular sail (Table 10)
 - Wind speed and centre of effort at 0.39 sail vertical span (DNVGL-ST-0412, 2016)

Table 10 – Moment comparison for triangular sails

Foundation height (m)	Sail height (m)		
	30	40	50
5	110%	111%	111%
10	110%	111%	112%
15	110%	111%	111%

There is a good level of accuracy, and the simplifications can be applied without major drawbacks for calculating the wind speed and its resultant pressure, force and moment on the sail for most cases. Even in the case of the rectangular sails, which underestimate slightly the results, this should not be a problem since other conservative assumptions are made along the wind force calculation. Naturally a more detailed analysis could utilize the integral of the wind pressure for the whole sail, considering the wind speed profile along the height, but, at

the same time it is the most accurate way to calculate such force, such procedure also requires much more effort.

Now that the height for wind speed assessment is defined, the forces generated by its action on sails can be discussed. Both lift and drag forces are considered in the fatigue analysis for WAPS. For traditional sails, the drag can be either insignificant or provide thrust according to the heading.

The lift force, L_A , and drag force, D_A , may be expressed as in equations 3 and 4:

$$L_A = \frac{1}{2} * \rho_{air} * V_A^2 * A * C_L \quad (3)$$

$$D_A = \frac{1}{2} * \rho_{air} * V_A^2 * A * C_D \quad (4)$$

Where A is the sail area, C_L is the lift coefficient and C_D is the drag coefficient. The air density ρ_{air} may be taken as 1.226 kg/m³ for dry air at 15°C, as in (DNV-RP-C205, 2019) [5.2.1].

The stress range is obtained for each wind speed-heading pair in the global wind matrix, combining this with WAPS data (coefficients, area, centre of effort). It considers the difference in the stresses from the mean wind speed amplified and reduced by the fatigue gust factor. The number of cycles for each stress range comes from the probability of occurrence of the speed-heading pair multiplied by the total number of cycles cumulated along the ship's lifetime.

4.2.7. Wind Correction due to Obstructions

Wind flow might be affected by other tall structures on deck or even by the ship's hull and superstructure. Such effect can be predicted with the aid of CFD calculations or wind tunnel tests; or, in a more simplified approach, it can be estimated by formulations of wind blowing past simplified geometries. However, it is acceptable to not consider this for the present calculations.

4.2.8. Induced Wind by Ship Motions

WAPS are affected by ship's pitch and roll motions, but it can be considered that they are not large, except for extreme rolling or pitching situations, when it is not recommended to utilize WAPS for safety reasons. Moreover, effects of such motions are accounted in the inertia loads. Therefore, the induced wind by them is not considered.

4.2.9. Shielding and Amplification Effects

The use of several sails in combination may induce both shielding, as one sail stays "behind" the other, but potentially also amplification effects. For the individual sail, it is however acceptable to disregard this effect. For more sails, the interaction between them can be estimated by CFD calculations or wind tunnel tests, what can be fundamental when defining the position of the sails on deck.

4.2.10. WAPS in Operational and Non-operation Modes

The purpose of the WAPS is to provide forward thrust and, so, it operates when there are favourable conditions. When, due to wind conditions, the WAPS does not provide this thrust or, even worse, it creates an unfavourable force relative to the ship route, the system is assumed to be in non-operation mode. However, it is still affected by fatigue loads.

This mode implies different actions according to the system, what affects the resulting forces on the WAPS. It can mean reefing (completely) the sail, folding it down, changing angle of sail system to minimize drag ("flag" or "idle" mode) or stopping revolutions of a rotating sail. Depending on the sail design, the non-operation mode may be dominated by inertial forces as the drag forces are expected to be small in this case.

Anyway, the effect of the non-operation mode shall be also accounted for in the fatigue calculations. This is also regarded as depending on heading and, thus, the apparent heading for such mode shall be evident in the calculations and in the operational profile. Moreover, even if small, the drag effects on the non-operating WAPS shall be included in the fatigue assessment.

However, the variety of WAPS also presents different operational modes, with different operational thresholds. These could be related, for example, to limiting the angle of attack or

reefing part of the sail, de-powering part of the sail to avoid lift and minimize drag, or having a sensor monitoring system to limit the forces on the foundations or limit acceleration levels. Therefore, adequate operational modes shall be defined in the operational profile for the fatigue calculations of each WAPS.

Regarding the operational profile, it is acceptable to be conservative in its definition from a fatigue assessment point of view. This simplifies the procedure for establishing the load history.

5. LOAD COMBINATION

The main challenge in assessing fatigue for WAPS is, however, to combine inertial and wind loads as the fatigue damage presents an exponential relation to the stress range. It is relatively simple to calculate the damage from each load, but the sum of the individual damages does not represent the total damage caused by both loads acting on the same time. Therefore, the stresses should be combined first and the damage assessed.

Such combination is performed in the context of the stress range spectrum. The load spectra from inertial and wind loads will be summed. Therefore, the load spectrum in terms of stress (or strain) shall be calculated for each load, as shown before, or chosen.

Three stress range spectra are considered relevant for this calculation: A, S7 and C. The straight-line spectrum A (Figure 27) should be used for inertia loads, but it may not be straight in the case Weibull slope is calculated (DNVGL-ST-0377, 2018) [4.6.5]. For the wind loads, the spectrum C represents a calculated spectrum up to a threshold, indicated by spectrum S7, up to which the wind loads are limited by the control system (Figure 28).

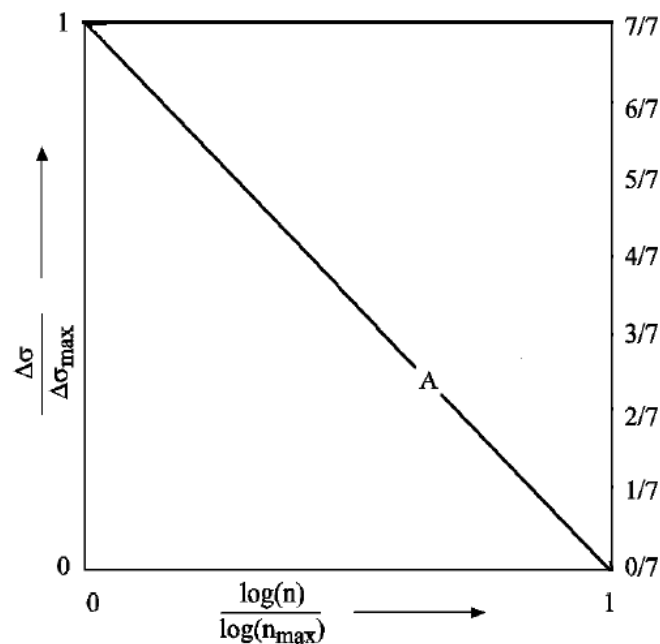


Figure 27 – Spectrum A for inertial loads, adapted from (DNVGL-ST-0377, 2018)

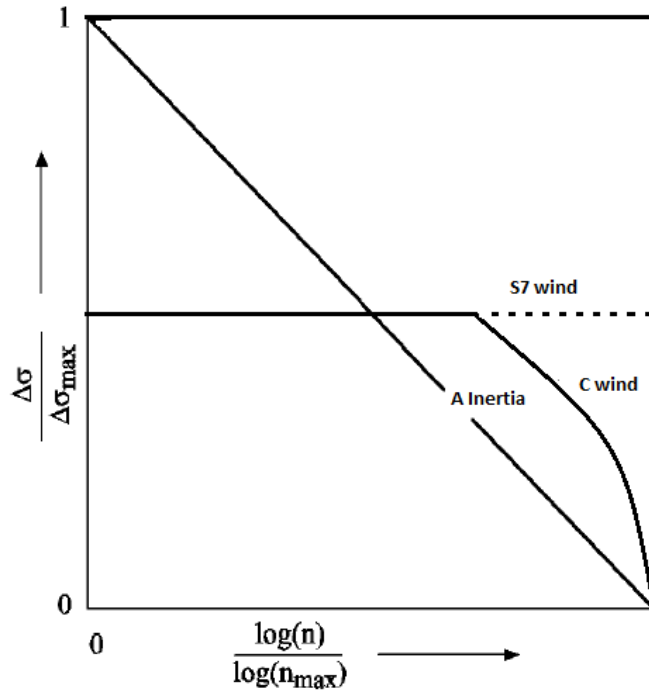


Figure 28 – Relevant stress range spectra, adapted from (DNVGL-ST-0377, 2018)

Spectra A and S7 are taken from (DNVGL-ST-0377, 2018) [4.6.5] (Figure 29), where spectrum A, considered out-of-operation condition for lifting appliances, is considered the in-operation condition for WAPS, since the latter does not operate when ship is not moving. Moreover, the control of the wind loads, keeping a constant stress range, fits S7.

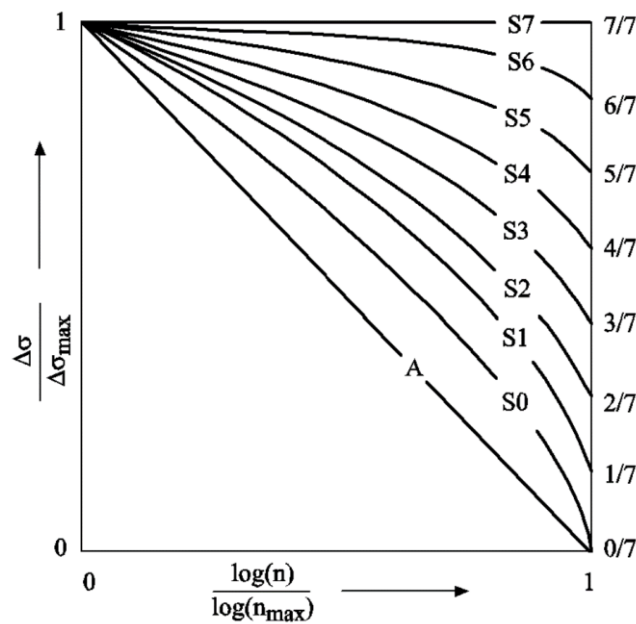


Figure 29 – Standard stress range spectra (DNVGL-ST-0377, 2018) [4.6.5]

Spectrum C is calculated from wind global matrix probability, applying the fatigue gust factor for the wind speeds in the matrix. Considering the WAPS's specific coefficients, it is possible to calculate the stresses and the stress range will be the difference between the maximum and minimum stress values, considering, respectively, the mean wind speed added or reduced by the factor. For wind loads with no practical upper limit on wind speed, the spectrum A may be used based on worst case scenario also for the highest design wind.

The number of cycles for each stress range is given by the probability of occurrence of each wind speed and heading. This probability is multiplied by the total number of fatigue cycles, which are calculated with basis on the roll period, T_θ , taken from (DNV-RU-SHIP Pt.3 Ch.4, 2021) Sec.3 [2.1.1], as exposed in equation 55:

$$T_\theta = \frac{2.3\pi k_r}{\sqrt{g GM}} \quad (55)$$

The total number of cycles also depends on the fraction time at sea, f_0 , which may vary according to the ship type. Then, the total number of cycles, n_0 , cumulated over the ship's lifetime is given by equation 66:

$$n_0 = \frac{f_0 \cdot T_{DF} \cdot 365.25 \cdot 24 \cdot 3600}{T_\theta} \quad (66)$$

Where T_{DF} is the minimum target design life, usually set for 25 years, which may be increased by the owner. Moreover, the roll radius of gyration, k_r , and the GM may be taken from (DNV-RU-SHIP Pt.3 Ch.9, 2021) Sec.4 [4.5] Table 2.

Therefore, the cycles are based on the roll period assumed to be the same as wind gust period and the gust amplification is based on this roll period. This, however, is not true for all the cases and the wind gust period may differ from the roll one. An alternative would be to establish time series for the wind and inertial loads from more advanced calculations and then, perform rainflow counting on the resulting broad band stress response to generate histogram and cycles.

Thus, the load combination can be performed in simple or more complex ways according to the level of information and the design phase. A central point in this step is the correlation between wind and wave, and how to consider their alignment (or misalignment) for this

analysis. A coarse procedure may be applied for assessing WAPS's general fatigue resistance, where a low level of detailing is required, while a more refined approach is useful for assessing damage for a specific feature.

In this sense, the level of complexity of different parameters, as number of cycles, load directional alignment and load magnitude, also needs to be discussed. The simplification of each one of them depends on the level of complexity adopted. In this sense, there are three approaches to combine wind and inertia loads:

- Simple superposition
- Simplified correlation
- Direct analysis

5.1. Load Combination Methods

5.1.1. Simple Superposition

Only the maximum wind and inertial loads, independent of relative heading, are considered. They are assumed to occur simultaneously as the worst possible combination. The stress range spectrum is established by adding the individual spectra integrally and this is used as basis for the fatigue calculation.

This method is conservative, but it may be a good option when looking for a robust design associated with low risks. More refined and optimized designs may present lighter weight, but this requires a more cautious structural analysis. The benefit of this weight reduction along the lifetime may be limited and, in that case, the increase in risk would not worth such effort.

5.1.2. Simplified Correlation

The wind and wave induced inertia may be assumed almost independent. At the same time, for simplification in this analysis, the true wind and the incident waves are assumed to act from the same direction. Therefore, the stress (load) history of the wind and the waves may be established for each heading separately and the combined stress for each stress block, $\Delta\sigma_i$, on the stress history may be calculated by equation 67:

$$\Delta\sigma_{i,tot} = \max(\Delta\sigma_{i,inertia} + 0.6\Delta\sigma_{i,wind}, 0.6\Delta\sigma_{i,inertia} + \Delta\sigma_{i,wind}) \quad (67)$$

The 0.6 factor is applied to the smaller load. This is based on (DNV CN 30.7, 2018), utilized for combining local and global stresses in the hull.

However, wind and waves distributions are generally represented in a different level of refinement. The wave headings are distributed along eight 45° sections (Figure 30) and the wind along seventy-two 5° sectors (Figure 31). So, the assumption that they act from the same direction means that, for each wave heading, nine wind headings are considered.

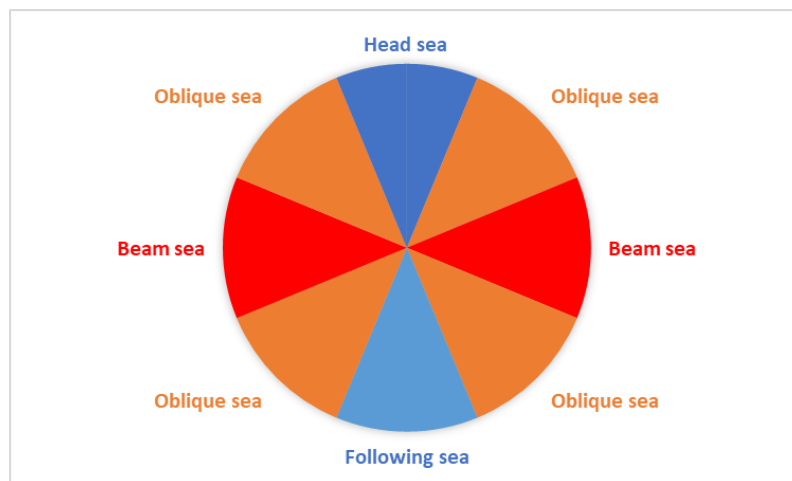


Figure 30 – Wave headings, 45° resolution (8 headings)

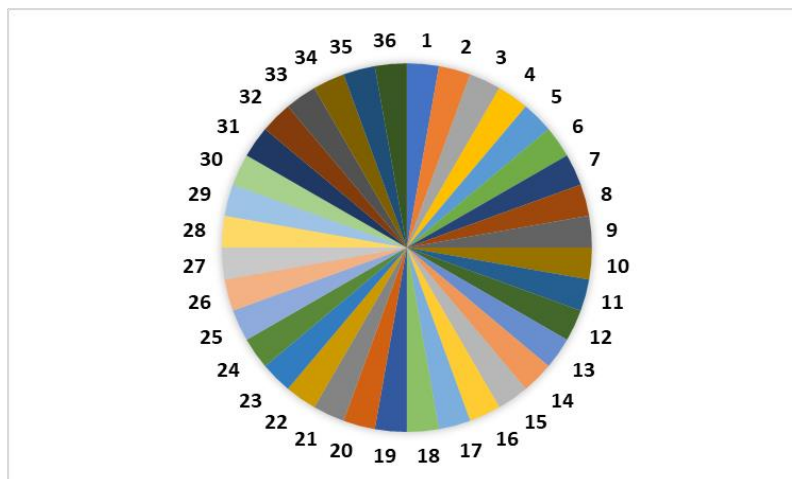


Figure 31 – Wind headings, 5° resolution (36 headings)

Moreover, each heading presents a probability, which should be considered for weighting the damage from each heading alignment in the total damage. It is important to notice that heading combination does not consider all wave headings and all wind ones at the same time.

The combination is performed by sectors, weighting the combined probability by the wind heading probability within that sector.

It can be explained in more details for better comprehension. Supposing wave headings evenly distributed, each one would present 12.5% probability of occurrence ($1/8$ of the total). Therefore, the sum of all wind-wave combinations in this sector is 12.5% and each combination can be weighted according to the wind distribution within this wave heading.

Therefore, if the wind probabilities for a given sector also sums 12.5% (evenly distributed), the probability of their combination with waves is not $1/8 \times 1/8$, but simply $1/8$, the probability of the wave heading. The relative probability of each wind heading within this interval would be $1/9$ and, so, the combined probability for each wind-wave set is $1/9 \times 1/8$. Now, it is easier to see that the probabilities sum $1/8$ for each wave heading and 1 for the whole group.

For the presented case, there are seventy-two combinations, logically, the same as the number of wind headings. The refinement of the wave headings just changes the number of wind headings considered within each one. By last, interpolation can be performed for not coincident intervals between wind and waves.

5.1.3. Direct Analysis

The last and more complex method is the direct analysis of the stress response, see (DNVGL-CG-0130, 2018). If wind and wave spectra are given, then the time series of a random realization of the stress response from the inertia and the wind can be generated and added for each heading. The result may be a broad banded process (even two peaked response spectrum) from which rainflow counting can be used to calculate the fatigue damage.

The probability between the wind and the waves may be taken from AIS based data matched with global environmental data where the wind data and the wave data can be retrieved jointly. Alternatively, the wind and wave data may be related through the Beaufort scale, considering randomness on the wave period.

For this method, the relation between the stress response at a specific location in the structure and the wave heading and frequency is expressed by stress transfer functions, which are combined to wave data and S-N curves to assess the fatigue damage. The transfer functions can be determined by component stochastic calculations, based on combining load transfer functions from wave or wind load analysis with stress factors, i.e., stress per unit load. Other

option is to utilize full stochastic analysis, where dynamic loads are directly transferred from the wave or wind load analysis program to FE models.

The procedure for wave loads can be found in (DNVGL-CG-0129, 2019) Sec.5 [3] and [4] (Figure 32 and Figure 33):

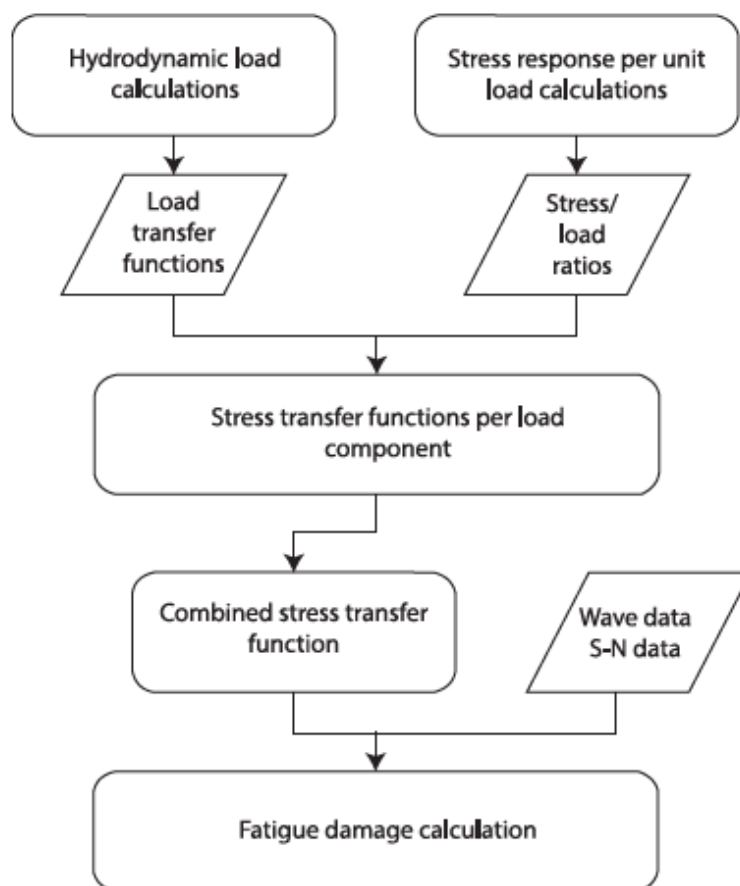


Figure 32 – Flow diagram for component stochastic fatigue calculations (DNVGL-CG-0129, 2019)

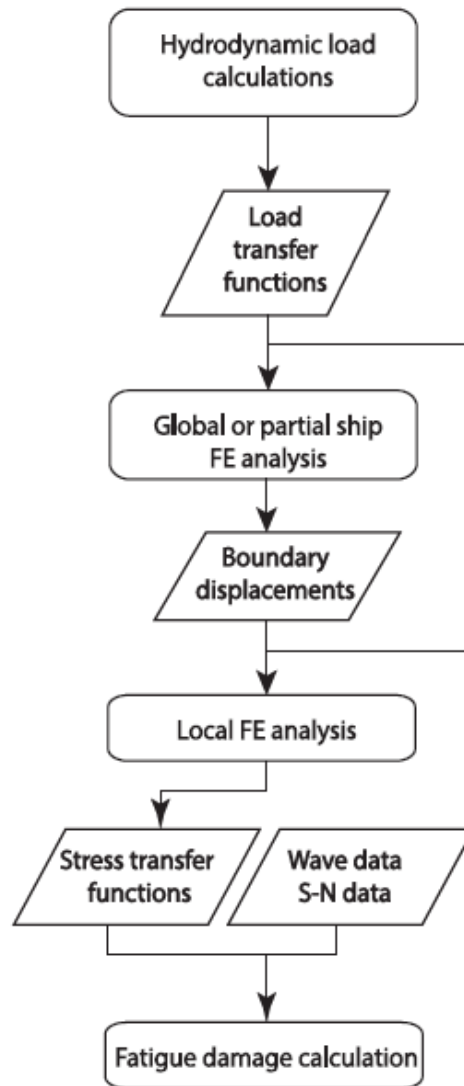


Figure 33 – Flow diagram for full stochastic fatigue calculations (DNVGL-CG-0129, 2019)

5.2. Stress Combination

The stresses shall be calculated for a specific hot spot separately for inertia and wind, then added according to the chosen method. Moreover, it shall be considered that moment for the wind and for the inertia act around different axis due to forward speed of the vessel and resulting direction of the wind load (combination of lift and drag). Stress magnitude varies with the distance to the axis, but it will always act along the vertical direction.

Regarding the alignment between wind and wave, inertia rules refer to North Atlantic while the global wind probability matrix refers to worldwide operation. This should be considered according to (DNV-RU-SHIP Pt.3 Ch.9, 2021). Therefore, the inertial loads shall be

combined with the environmental factor $f_e = 0.8$ for worldwide wave environment, taken from Section 4, [4.2].

Moreover, many WAPS rotate according to the wind conditions and, so, the hot spots below and above the rotational bearing may experience quite different loading. The hot spots below the bearing are fixed to the ship coordinate system, while hot spots above are fixed to the mast coordinate system. Both shall be considered, with the suitable load conversions when needed.

6. FATIGUE ASSESSMENT FOR WAPS

At this point, after defining how loads and stresses should be approached, the ideal would be to perform the whole procedure through its different approaches, comparing the results according to the level of detail adopted. Moreover, such results should be compared to the most precise result, what would mean a rainflow counting of running stress time series from random realisations of wind speed with gusts and turbulence combined with the wave motions applied to a moving ship. This would need to cover all relevant wind speeds and headings in a wind scatter diagram, relevant vessel speeds and headings relative to the waves in a complete wave scatter diagram, also accounting for swells.

Such analyses, however, consume a considerable amount of time and require a large amount of information, including details of the WAPS operation. Besides, the approaches established here also aim to avoid going into very detailed analyses when it is not necessary, working at different levels of complexity to allow the calculation of a rough estimation as well as of a refined result.

Furthermore, in the sense of validation, many steps in the procedures required a validation in themselves. This was a constant when dealing with wind loads for ships, especially when it comes to the wind speed profile and gusts. The assumptions and calculations required were justified along the path to build the final set of procedures and, therefore, it is possible to summarize them to comprise the whole developed approach and provide a better understanding of it.

To begin with, the analysis require data from ship (as main dimensions and other information), from the WAPS (dimensions, aerodynamic coefficients, operational profile, location on deck, hot spots) and from the weather (wind and wave global distribution or scatter diagrams). With ships main dimensions and utilization rate of the system, it is possible to calculate the roll period (equation 55) and the total number of cycles (equation 66) along the lifetime of the WAPS:

$$T_{\theta} = \frac{2.3\pi k_r}{\sqrt{g} GM} \quad (55)$$

$$n_0 = \frac{f_0 \cdot T_{DF} \cdot 365.25 \cdot 24 \cdot 3600}{T_{\theta}} \quad (66)$$

Then, before calculating the stresses for the wind-wave combinations, it is necessary to define the number of cycles experienced at each wind-wave combination. This depends, naturally, on the load combination method utilized. It can be done as the simplified correlation (5.1.2), for example, for which wind-wave combinations are weighted according to the probability of each wind heading within a wave heading.

The number of cycles is obtained for each wind heading within the wave heading. However, for assessing fatigue stress load, it is also necessary to consider hot spots in the support structure. The stress ranges and spectra must be calculated for each one of them.

The stress range can be calculated in two separated parts: inertial loads and wind loads. Beginning with the inertial loads, they can be calculated in different ways:

- Envelope accelerations (4.1.1)
- Equivalent design approach (4.1.2)
- Direct hydrodynamics calculation (4.1.3)

The stress range for the S-N curves needs to be corrected for the factors presented in (3.2), as showed in equation 10:

$$\Delta\sigma_{FS} = f_{mean} \cdot f_{thick} \cdot f_{material} \cdot f_w \cdot f_c \cdot f_s \cdot K_m \cdot \Delta\sigma \quad (10)$$

The stress arising from wind loads can be calculated as explained in (4.2), with the adequate fatigue gust factor, G_R , calculated by equation 65 shown in (4.2.3). If the wind speed is higher than 15m/s, a safety factor of 0.01 is added to equation 65:

$$G_R(U_0, T_\theta) = (2,44 * \ln(U_0) + 0,14T_\theta) * 10^{-2} \quad (65)$$

Alternatively, the procedure utilized for calculating the fatigue gust factor can be replicated for the WAPS in question.

Then, the stress spectra must be combined into a single stress spectrum, according to the methods exposed in (5.1), considering the points in (5.2):

- Simple superposition
- Simplified correlation
- Direct analysis

The combined single stress spectrum allows to assess the fatigue damage as exposed in (3.3.2), in the context of each hot spot individually.

Such steps are performed for each hot spot in a determined wind heading within a wave heading. Therefore, the damages for each hot spot should be added for all the prescribed combinations, what means summing the damages for each hot spot for each wind heading within each one of the wave headings. As the number of cycles was already adjusted for the probability of each one of these combinations, the sum of the damages delivers the final fatigue damage for each hot spot, which should be compared to the cumulative damage given by the design fatigue factor.

7. CONCLUSION

At first, the thesis aimed to provide a good basis for the fatigue assessment for WAPS. For such, there was a review of the physics behind sailing (2.1), explaining how WAPS work and giving an overview of the different systems (2.2). Moreover, the rules developed so far were presented and their limitations were explained (2.3.1).

In this sense, the problem was compared to the challenges faced by the offshore wind area, enlarging the understanding about the theme (2.3.2). Then different aspects were attacked in order to narrow the scope for necessary approach, developed for the WAPS supports (2.3.3).

In the sequence, the general procedure for assessing fatigue damage was presented to stress the relevant points to be worked while considering inertial and wind loads: the stress range necessary for the stress spectra and the number of cycles (Chapter 3). These points were attacked in Chapter 4 and their combination was the focus in Chapter 5, in the work for building the assumptions for a feasible fatigue approach.

For this, the main achievement of the thesis was to develop an approach for assessing fatigue for WAPS, presenting points to be added to previous standards, as (DNVGL-ST-0511, 2019).

This was based on different rules, recommended practices and standards, especially:

- (DNV-RU-SHIP Pt.3 Ch.4, 2021) – wave loads.
- (DNV-RP-C205, 2019) – weather loads, mainly wind loads, which needed to be adapted for fatigue.
- (DNV-RU-SHIP Pt.3 Ch.9, 2021) and (DNVGL-CG-0129, 2019) – fatigue assessment of hull and ship structures.
- (DNVGL-ST-0377, 2018) – lifting appliances, due to their similarity regarding the wind action.

Such correlation with established guidelines is very useful in the sense that designers can base their work on previous knowledge, not requiring a totally new learning. This eases the understanding and application of the new approach.

Regarding the results, the wind load application was established based on (DNVGL-ST-0412, 2016), proving that simplifications can be utilized without major problems or can even be slightly to the safe side (in case of triangular sails), as seen in (4.2.6). The other assumptions for assessing wind speed were also drawn to facilitate the analysis.

However, the main contribution of the present work was to develop not only a fatigue gust factor, but also a procedure which allows its calculation to be adapted for different systems,

even utilizing different materials and S-N curves (4.2.3). This was achieved through the exploration of wind profiles and spectra suited for offshore wind. The results delivered by the proposed formula agreed with the ones delivered by wind stress series in time

This, in combination with wave loads, complemented the whole comprehension of fatigue loads and stresses necessary for assessing the fatigue damage, leaving just the task of combining such loads in the hot spots frame. For such task, both a simple and a rather complex methods could be achieved without large difficulties. The challenge, however, was to develop a simplified correlation between wind and waves for accounting the different alignments between them (5.1.2) in a credible, but not too complex, way.

In the end, a summary for the whole procedure was presented to allow a global view of the developed approach and its application. However, it still lacks a thorough comparison between the proposed approach, at its different detail levels, and the most precise results possible, to be obtained through the application of stress time series from combined wind and wave data for a navigating ship, with stresses and fatigue damage assessed through rainflow.

For future works, it is suggested to carry such comparisons between the approach established and time domain analyses in order to find any points to be enhanced in the procedure. Still at this point, finding a way to simplify the combination of winds and waves for navigating ships is also a task to be achieved. These two points need to account for different wind and wave headings, their magnitudes, the vessel speed and WAPS operation for different weather conditions.

Nevertheless, the present work represents a first step towards a consolidated fatigue approach for WAPS. It is expected that such systems continue to be developed and adopted by the ship industry as a reliable way to reduce CO₂ and GHG emissions. In such case, this work can be, at least, a basis for establishing fatigue assessment methodologies for WAPS in the future.

8. ACKNOWLEDGEMENTS

At first, I would like to thank my supervisor, Jörg Peschmann, along with Hasso Hoffmeister and Gaute Storhaug, for their inestimable support, contribution and guidance during the entire development of this thesis. Their insights, critics and suggestions were fundamental for this work. I also thank DNV for the opportunity of working in such a challenging and novel topic. Besides, this would not happen without the effort of many people that make the EMSHIP program possible. For this, I thank especially Prof. Philippe Rigo, Prof. Robert Bronsart and Dr. Thomas Lindemann for the dedication to the program. This acknowledgement is extended to the staffs from the universities of Liège and Rostock for all their commitment.

I also need to express my gratitude to my parents Elisabeth and Armando for the support along my whole life, as well as to my godparents José and Emilia, who believe in and support the education of the whole family.

A special thanks to my girlfriend Carolina for standing by me along the two years of the master's course, among short and long distances, quarantines and travel restrictions.

By last, I would like to thank the Federal University of Rio de Janeiro (UFRJ) for the whole knowledge acquired there and specially for believing that education should be a right and not a privilege.

9. REFERENCES

- Ayro. (2021). *Projects*. Retrieved July 30, 2021, from Ayro: <http://ayro.fr/projects/>
- Benitz, M., Lackner, M., & Schmidt, D. (2015). Hydrodynamics of offshore structures with specific focus on wind energy applications. *Renewable and Sustainable Energy Reviews*, Vol 44, pp. 692-716.
- Bordogna, G. (2020). *Aerodynamic of Wind-Assisted Ships - Interaction effects on the aerodynamic performance of multiple wind-propulsion systems*. PhD Thesis, Delft University of Technology.
- DNV. (2020, January 8). *Wind ships ahead*. Retrieved from DNV - Maritime Impact: <https://www.dnv.com/expert-story/maritime-impact/Wind-ships-ahead.html>
- DNV CN 30.7. (2018). *Fatigue Assessment of Ship Structures*.
- DNV-GL. (2020). *Wind Propulsion*. Høvik, Norway.
- DNVGL-CG-0129. (2019). *Class Guideline, Fatigue assessment of ship structures*.
- DNVGL-CG-0130. (2018). *Class Guideline, Wave Loads*.
- DNVGL-ST-0377. (2018). *Standard; Shipboard lifting appliances*.
- DNVGL-ST-0412. (2016). *Standard, Design and construction of large modern yacht rigs*.
- DNVGL-ST-0511. (2019). *Standard, Wind assisted propulsion systems*.
- DNV-RP-C205. (2019). *Recommended Practice, Environmental conditions and environmental loads*.
- DNV-RU-SHIP Pt.3 Ch.4. (2021). *Rules for Classification, Ships, Part 3 - Hull, Chapter 4 – Loads*.
- DNV-RU-SHIP Pt.3 Ch.9. (2021). *Rules for Classification, Ships, Part 3 – Hull, Chapter 9 – Fatigue*.
- DNV-RU-SHIP Pt.6 Ch.2. (2021). *Rules for Classification, Ships, Part 6 - Additional class notations, Chapter 2 - Propulsion, power generation and auxiliary systems*.
- Dong, W., Moan, T., & Gao, Z. (2011). Long-term fatigue analysis of multi-planar tubular joints for jacket-type offshore wind turbine in time domain. *Engineering Structures*, Vol 33(6), pp. 2002-2014.
- Dykstra. (n.d.). *WASP (Ecoliner)/Sailing cargo ship*. Retrieved July 29, 2021, from <https://www.dykstra-na.nl/designs/wasp-ecoliner/>
- eConowind. (2021). Retrieved July 29, 2021, from ECONOWIND: <https://www.econowind.nl/>

- ENERCON. (2013). Retrieved July 29, 2021, from ENERCON: https://www.enercon.de/fileadmin/Redakteur/Medien-Portal/windblatt/pdf/WB_03-2013_deu_web.pdf
- Fakiolas, K. M. (2020). *Wind Propulsion Principles*.
- Fricke, W. (2017). Fatigue and Fracture of Ship Structures. In *Encyclopedia of Maritime and Offshore Engineering*. John Wiley & Sons, Ltd.
- Fricke, W., Petershagen, H., & Paetzold, H. (1997). *Fatigue Strength of Ship Structures; Part I – Basic Principles*.
- Hodgson, T., Sampathkumar, N., & Cortizo, I. (2016). Approach to wind wave correlation in coupled analysis of offshore WTG substructures. *Wind Europe Summit*.
- IMO. (2021). *Greenhouse Gas Emissions*. Retrieved July 29, 2021, from International Maritime Organization: <https://www.imo.org/en/OurWork/Environment/Pages/GHG-Emissions.aspx>
- IMO Environmental Committee. (2021). *Initial IMO GHG Strategy*. Retrieved July 29, 2021, from International Maritime Organization (IMO): <https://www.imo.org/en/MediaCentre/HotTopics/Pages/Reducing-greenhouse-gas-emissions-from-ships.aspx>
- Lee, T., & Tjhung, T. (2012). Chapter 3 - Rainflow Cycle Counting Techniques. In *Metal Fatigue Analysis Handbook* (pp. 89-114). Butterworth-Heinemann.
- Li, X., Zhu, C., Fan, Z., Chen, X., & Jianjun Tan. (2020). Effects of the yaw error and the wind-wave misalignment on the dynamic characteristics of the floating offshore wind turbine. *Ocean Engineering*, Vol 199.
- Maltese Falcon. (2020). Retrieved July 29, 2021, from Maltese Falcon: <http://www.symaltesefalcon.com/brochure.php>
- Marchaj, C. A. (1982). Aerodynamik und Hydrodynamic des Segelns (Aerodynamics and Hydrodynamics of Sailing).
- Marghany, M. (2020). Chapter 6 - Quantum description of sea surface. In *Synthetic Aperture Radar Imaging Mechanism for Oil Spills* (pp. 93-110). Gulf Professional Publishing.
- Marine Environment Protection Committee. (2011). *Reduction of GHG emissions from ships - Global Wind Specification along the Main Global Shipping Routes to be applied in the EEDI calculation of wind propulsion systems*.
- Mathis Ruhl Architecture Navale. (n.d.). *Wind Motion 120*. Retrieved from Mathis Ruhl.
- MathWorks. (n.d.). *Rainflow*. Retrieved July 29, 2021, from MathWorks Help Center: <https://de.mathworks.com/help/signal/ref/rainflow.html>

- Michelin. (2021). *2021 Movin'On: Michelin presents two innovations to accelerate the development of sustainable mobility*. Retrieved July 30, 2021, from Michelin: <https://www.michelin.com/en/press-releases/2021-movinon-michelin-presents-two-innovations-to-accelerate-the-development-of-sustainable-mobility/>
- NauticEd. (2013). *Americas Cup Apparent Wind*. Retrieved from NauticEd: <https://www.nauticed.org/sailing-blog/americas-cup-apparent-wind/>
- Norsepower. (2020). *Passenger vessel*. Retrieved July 29, 2021, from Norsepower: <https://www.norsepower.com/passenger/>
- Norsepower. (2018). *Tankers*. Retrieved July 30, 2021, from Norsepower: <https://www.norsepower.com/tankers/>
- Ovcina, J. (2021, March 2). *Windship Technology's true zero-emission ship design sparks interest from the market*. Retrieved July 30, 2021, from Offshore Energy: <https://www.offshore-energy.biz/windship-technologys-true-zero-emission-ship-design-sparks-interest-from-the-market/>
- Püschl, W. (2018). High-speed sailing. *European Journal of Physics*, Vol 39.
- Reche, M. (2020). *Performance Prediction Program for Wind-Assisted Cargo Ships*. Master's Thesis, DTU (Technical University of Denmark), Department of Mechanical Engineering.
- United Nations. (2021). *Facts about the Climate Emergency*. Retrieved July 29, 2021, from UN Environment Programme: <https://www.unep.org/explore-topics/climate-change/facts-about-climate-emergency>
- Verma, A., Jiang, Z., Ren, Z., & Gao, Z. &. (2020). Effects of Wind-Wave Misalignment on a Wind Turbine Blade Mating Process: Impact Velocities, Blade Root Damages and Structural Safety Assessment. *Journal of Marine Science and Application*, Vol 19, 218–233.
- World Meteorological Organisation. (2008). *Guidelines for Converting Between Various Wind Averaging Periods in Tropical Cyclone Conditions*.
- Yeter, B., Garbatov, Y., & Guedes Soares, C. (2013). Spectral fatigue assessment of an offshore wind turbine structure under wave and wind loading. In *Developments in Maritime Transportation and Exploitation of Sea Resources* (pp. 425-433). London, UK: Francis & Taylor Group.

ANNEX

Table 11 – Normalized global wind chart showing the probability of wind conditions relative to the ship's heading along the main global trading routes

W/Ind Angle [°] W/Ind Speed [m/s]		0	5	10	15	20	25	30	35	40	45	50	55	60	65	70	75	80	85	90	95	100	105	110	115
<1	0.0001	0.0001	0.0001	0.0001	0.0001	0.0001	0.0001	0.0001	0.0001	0.0001	0.0001	0.0001	0.0001	0.0001	0.0001	0.0001	0.0001	0.0001	0.0001	0.0001	0.0001	0.0001	0.0001	0.0001	0.0001
<2	0.0005	0.0005	0.0005	0.0005	0.0005	0.0005	0.0005	0.0005	0.0005	0.0005	0.0005	0.0005	0.0005	0.0005	0.0005	0.0005	0.0005	0.0005	0.0005	0.0005	0.0005	0.0005	0.0005	0.0005	0.0005
<3	0.0009	0.0009	0.0009	0.0009	0.0009	0.0008	0.0008	0.0008	0.0008	0.0008	0.0008	0.0008	0.0008	0.0008	0.0008	0.0008	0.0008	0.0008	0.0008	0.0008	0.0008	0.0008	0.0008	0.0008	0.0008
<4	0.0013	0.0013	0.0013	0.0013	0.0012	0.0012	0.0012	0.0012	0.0011	0.0011	0.0011	0.0011	0.0011	0.0011	0.0011	0.0011	0.0010	0.0010	0.0010	0.0010	0.0011	0.0011	0.0011	0.0011	0.0011
<5	0.0017	0.0017	0.0016	0.0016	0.0015	0.0015	0.0015	0.0014	0.0014	0.0014	0.0013	0.0013	0.0013	0.0013	0.0012	0.0012	0.0012	0.0012	0.0012	0.0013	0.0013	0.0013	0.0013	0.0013	0.0013
<6	0.0021	0.0020	0.0020	0.0019	0.0018	0.0018	0.0017	0.0016	0.0016	0.0015	0.0015	0.0014	0.0014	0.0014	0.0014	0.0014	0.0013	0.0014	0.0014	0.0014	0.0014	0.0014	0.0014	0.0015	0.0015
<7	0.0022	0.0022	0.0021	0.0020	0.0020	0.0019	0.0018	0.0017	0.0017	0.0016	0.0015	0.0014	0.0014	0.0014	0.0014	0.0014	0.0014	0.0014	0.0014	0.0014	0.0014	0.0015	0.0015	0.0015	0.0015
<8	0.0020	0.0020	0.0020	0.0019	0.0019	0.0018	0.0017	0.0016	0.0016	0.0015	0.0014	0.0014	0.0013	0.0013	0.0013	0.0013	0.0013	0.0013	0.0013	0.0013	0.0013	0.0013	0.0014	0.0014	0.0014
<9	0.0017	0.0017	0.0017	0.0016	0.0016	0.0016	0.0015	0.0014	0.0014	0.0013	0.0013	0.0012	0.0012	0.0011	0.0011	0.0011	0.0011	0.0011	0.0011	0.0011	0.0011	0.0011	0.0011	0.0012	0.0012
<10	0.0013	0.0013	0.0013	0.0013	0.0013	0.0013	0.0012	0.0012	0.0011	0.0011	0.0010	0.0010	0.0010	0.0010	0.0009	0.0009	0.0009	0.0009	0.0009	0.0009	0.0008	0.0008	0.0008	0.0009	0.0009
<11	0.0010	0.0010	0.0010	0.0010	0.0009	0.0009	0.0009	0.0009	0.0009	0.0008	0.0008	0.0008	0.0008	0.0008	0.0007	0.0007	0.0007	0.0007	0.0006	0.0006	0.0006	0.0006	0.0006	0.0006	0.0006
<12	0.0007	0.0007	0.0007	0.0007	0.0006	0.0006	0.0006	0.0006	0.0006	0.0006	0.0005	0.0005	0.0005	0.0005	0.0005	0.0005	0.0005	0.0005	0.0004	0.0004	0.0004	0.0004	0.0004	0.0004	0.0004
<13	0.0004	0.0005	0.0005	0.0005	0.0004	0.0004	0.0004	0.0004	0.0004	0.0004	0.0004	0.0003	0.0003	0.0003	0.0003	0.0003	0.0003	0.0003	0.0003	0.0003	0.0003	0.0002	0.0002	0.0002	0.0002
<14	0.0003	0.0003	0.0003	0.0003	0.0003	0.0003	0.0003	0.0003	0.0003	0.0003	0.0002	0.0002	0.0002	0.0002	0.0002	0.0002	0.0002	0.0002	0.0002	0.0002	0.0002	0.0002	0.0002	0.0002	0.0002
<15	0.0002	0.0002	0.0002	0.0002	0.0002	0.0002	0.0002	0.0002	0.0002	0.0002	0.0002	0.0002	0.0002	0.0001	0.0001	0.0001	0.0001	0.0001	0.0001	0.0001	0.0001	0.0001	0.0001	0.0001	0.0001
<16	0.0001	0.0001	0.0001	0.0001	0.0001	0.0001	0.0001	0.0001	0.0001	0.0001	0.0001	0.0001	0.0001	0.0001	0.0001	0.0001	0.0001	0.0001	0.0001	0.0001	0.0001	0.0001	0.0001	0.0001	0.0001
<17	0.0001	0.0001	0.0001	0.0001	0.0001	0.0001	0.0001	0.0001	0.0001	0.0001	0.0001	0.0001	0.0001	0.0001	0.0001	0.0001	0.0001	0.0001	0.0001	0.0001	0.0001	0.0001	0.0001	0.0001	0.0001
<18	0.0001	0.0001	0.0001	0.0001	0.0001	0.0001	0.0001	0.0001	0.0000	0.0000	0.0000	0.0000	0.0000	0.0000	0.0000	0.0000	0.0000	0.0000	0.0000	0.0000	0.0000	0.0000	0.0000	0.0000	0.0000
<19	0.0000	0.0000	0.0000	0.0000	0.0000	0.0000	0.0000	0.0000	0.0000	0.0000	0.0000	0.0000	0.0000	0.0000	0.0000	0.0000	0.0000	0.0000	0.0000	0.0000	0.0000	0.0000	0.0000	0.0000	0.0000
<20	0.0000	0.0000	0.0000	0.0000	0.0000	0.0000	0.0000	0.0000	0.0000	0.0000	0.0000	0.0000	0.0000	0.0000	0.0000	0.0000	0.0000	0.0000	0.0000	0.0000	0.0000	0.0000	0.0000	0.0000	0.0000
<21	0.0000	0.0000	0.0000	0.0000	0.0000	0.0000	0.0000	0.0000	0.0000	0.0000	0.0000	0.0000	0.0000	0.0000	0.0000	0.0000	0.0000	0.0000	0.0000	0.0000	0.0000	0.0000	0.0000	0.0000	0.0000
<22	0.0000	0.0000	0.0000	0.0000	0.0000	0.0000	0.0000	0.0000	0.0000	0.0000	0.0000	0.0000	0.0000	0.0000	0.0000	0.0000	0.0000	0.0000	0.0000	0.0000	0.0000	0.0000	0.0000	0.0000	0.0000
<23	0.0000	0.0000	0.0000	0.0000	0.0000	0.0000	0.0000	0.0000	0.0000	0.0000	0.0000	0.0000	0.0000	0.0000	0.0000	0.0000	0.0000	0.0000	0.0000	0.0000	0.0000	0.0000	0.0000	0.0000	0.0000
<24	0.0000	0.0000	0.0000	0.0000	0.0000	0.0000	0.0000	0.0000	0.0000	0.0000	0.0000	0.0000	0.0000	0.0000	0.0000	0.0000	0.0000	0.0000	0.0000	0.0000	0.0000	0.0000	0.0000	0.0000	0.0000
<25	0.0000	0.0000	0.0000	0.0000	0.0000	0.0000	0.0000	0.0000	0.0000	0.0000	0.0000	0.0000	0.0000	0.0000	0.0000	0.0000	0.0000	0.0000	0.0000	0.0000	0.0000	0.0000	0.0000	0.0000	0.0000
>=25	0.0000	0.0000	0.0000	0.0000	0.0000	0.0000	0.0000	0.0000	0.0000	0.0000	0.0000	0.0000	0.0000	0.0000	0.0000	0.0000	0.0000	0.0000	0.0000	0.0000	0.0000	0.0000	0.0000	0.0000	0.0000

